Supporting Information for

Fluorescent Oxazoles from Quinones for Bioimaging Applications

Gleiston G. Dias,[a] Pamella V. B. Pinho,[a] Hélio A. Duarte,[a] Jarbas M. Resende,[a] Andressa B. B. Rosa,[b] José R. Correa,[b] Brenno A. D. Neto[b]* and Eufrânio N. da Silva Júnior[a]*

[a]Institute of Exact Sciences, Department of Chemistry, Federal University of Minas Gerais, Belo Horizonte, 31270-901, MG, Brazil.
[b]Laboratory of Medicinal & Technological Chemistry, Institute of Chemistry, University of Brasilia, P.O. Box 4478, Brasilia, 70904970, DF, Brazil.

E-mail: eufranio@ufmg.br, brenno.ipi@gmail.com

Contents

NMR assignments

The assignments of ^{1}H and ^{13}C resonances of the compounds **P1-P4** were performed by the combined analysis of the respective 1D and 2D COSY, ^{1}H-^{13}C HSQC and ^{1}H-^{13}C HMBC spectra. While multiplicity of all ^{1}H signals as well as the respective ^{1}H-^{1}H scalar coupling constants and the COSY correlations are in agreement with aromatic and aliphatic ^{1}H spin systems, the assignment of the carbon resonances was accessed by analysis of the HSQC and HMBC contour maps (see Tables S1 to S4 and Figures S1 to S36).

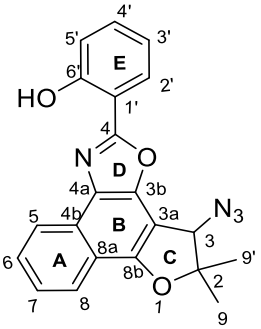

Table S1. ^{1}H and ^{13}C NMR data of **P1** in $CDCl_3$ at 303 K

(^{1}H and ^{13}C data recorded at 400 and 100 MHz, respectively)

Index	δ ^{13}C/ppm	δ ^{1}H(m)/ppm *a*	^{n}J/Hz *b*	COSY (n) *b,c*	HMBC (n) *b,c*
2	91.4	-	-	-	9/9'(2)
3	69.4	5.13 (s)	-	-	9/9'(3)
4	160.6	-	-	-	2'(3), 5'(4,w)
5	122.5	8.44 (ddd)	$^{3}J_{H5-H6}$ 8.3, $^{4}J_{H5-H7}$ 1.2, $^{5}J_{H5-H8}$ 0.8	6(3), 7(4w), 8(5w)	6(2), 7(3), 8(4), 3(6w)
6	128.6	7.71 (ddd)	$^{3}J_{H5-H6}$ 8.3, $^{3}J_{H6-H7}$7.0, $^{4}J_{H6-H8}$ 1.2	5(3), 7(3), 8(4w)	5(2), 7(2), 8(3)
7	125.4	7.55 (ddd)	$^{3}J_{H6-H7}$ 7.0, $^{3}J_{H7-H8}$ 8.3, $^{4}J_{H5-H7}$ 1.2	6(3), 8(3), 5(4w)	8(2w), 5(3)
8	123.4	8.11 (ddd)	$^{3}J_{H7-H8}$ 8.3, $^{4}J_{H6-H8}$ 1.2, $^{5}J_{H5-H8}$ 0.8	7(3), 6(4w), 5(5w)	7(2), 6(3), 5(4), 3(5w)
9/9'	22.3/27.4	1.73 (s)/1.58 (s)	-	9'(4)/9(4)	3(3), 9'(3)/3(3), 9(3)
3a	102.7	-	-	-	3(2)
3b	143.2	-	-	-	3(3)
4a	130.1	-	-	-	5(3), 3(4w), 8(4w)
4b	126.6	-	-	-	5(2), 6(3), 8(3), 3(5w)
8a	119.1	-	-	-	8(2w), 5(3), 7(3), 3(4w), 6(4w)
8b	155.5	-	-	-	3(3), 8(3), 5(4w)
1'	111.1	-	-	-	3'(3), 5'(3), OH(3w), 4'(4w)
2'	126.5	8.06 (ddd)	$^{3}J_{H2'-H3'}$ 7.9, $^{4}J_{H2'-H4'}$ 1.7, $^{5}J_{H2'-H5'}$ 0.4	3'(3), 4'(4)	3'(2), 4'(3)
3'	119.7	7.03 (ddd)	$^{3}J_{H2'-H3'}$ 7.9, $^{3}J_{H3'-H4'}$ 7.3, $^{4}J_{H3'-H5'}$ 1.1	2'(3), 4'(3)	5'(3)
4'	132.7	7.42 (ddd)	$^{3}J_{H3'-H4'}$ 7.3, $^{3}J_{H4'-H5'}$ 8.3, $^{4}J_{H2'-H4'}$ 1.7	3'(3), 5'(3), 2'(4)	3'(2), 2'(3)
5'	117.3	7.15 (ddd)	$^{3}J_{H4'-H5'}$ 8.3, $^{4}J_{H3'-H5'}$ 1.1, $^{5}J_{H2'-H5'}$ 0.4	4'(3)	4'(2), 3'(3), OH(3), 2'(4w),
6'	157.7	-	-	-	5'(2w), OH(2w), 2'(3), 4'(3), 3'(4w)
OH	-	11.38 (s)	-	-	-

a – m = multiplicity; *b* – n = number of chemical bonds; *c* – "w" means week intensity correlation

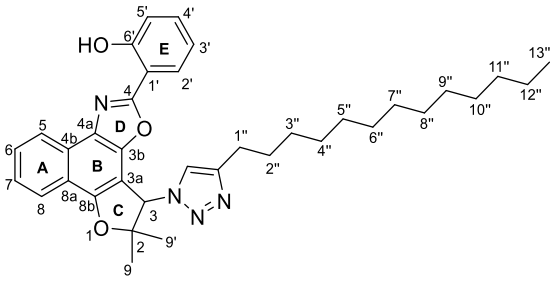

Table S2. ^{1}H and ^{13}C NMR data of **P2** in $CDCl_3$ at 303 K

(^{1}H and ^{13}C data recorded at 400 and 100 MHz, respectively)

Index	δ^{13}C/ppm	δ^{1}H(m)/ppm [a]	^{n}J/Hz [b]	COSY (n) [b,c]	HMBC (n) [b,c]
2	91.9	-	-	-	3(2w), 9(2), 9'(2), $5_{triazole}$(4w)
3	68.1	6.47 (s)	-	$5_{triazole}$(4w)	9(3), 9'(3), $5_{triazole}$(3)
4	160.9	-	-	-	2'(3), 5'(4)
5	122.6	8.48 (ddd)	$^{3}J_{H5\text{-}H6}$ 8.3, $^{4}J_{H5\text{-}H7}$ 1.2, $^{5}J_{H5\text{-}H8}$ 0.8	6(3), 7(4w), 8(5w)	7(3), 8(4w)
6	129.1	7.78 (ddd)	$^{3}J_{H5\text{-}H6}$ 8.3, $^{3}J_{H6\text{-}H7}$ 7.0, $^{4}J_{H6\text{-}H8}$ 1.2	5(3), 7(3), 8(4w)	5(2w), 7(2w), 8(3)
7	125.8	7.62 (ddd)	$^{3}J_{H6\text{-}H7}$ 7.0, $^{3}J_{H7\text{-}H8}$ 8.3, $^{4}J_{H5\text{-}H7}$ 1.2	6(3), 8(3), 5(4w)	8(2w), 5(3)
8	123.5	8.19 (ddd)	$^{3}J_{H7\text{-}H8}$ 8.3, $^{4}J_{H6\text{-}H8}$ 1.2, $^{5}J_{H5\text{-}H8}$ 0.8	7(3), 6(4w), 5(5w)	7(2w), 6(3), 5(4w), 3(5w)
9/9'	21.1/27.3	1.10-1.33 (m)/1.76 (s)	-	9'(4)/9(4)	3(3), 9'(3)/3(3), 9(3)
3a	101.3	-	-	-	3(2), 8(4w), 7(5w),
3b	142.6	-	-	-	3(3), 5(4w), 6(5w)
4a	130.6	-	-	-	5(3), 3(4w), 8(4w)
4b	126.9	-	-	-	5(2), 6(3), 8(3), 7(4w), 3(5w)
8a	119.1	-	-	-	8(2w), 5(3), 7(3), 3(4w), 6(4w)
8b	156.1	-	-	-	3(3), 8(3), 5(4w)
1'	110.7	-	-	-	3'(3), 5'(3), OH(3w), 4'(4w)
2'	126.6	7.87 (ddd)	$^{3}J_{H2'\text{-}H3'}$ 7.9, $^{4}J_{H2'\text{-}H4'}$ 1.7, $^{5}J_{H2'\text{-}H5'}$ 0.4	3'(3), 4'(4), 5'(5w)	3'(2), 4'(3)
3'	119.7	6.96 (ddd)	$^{3}J_{H2'\text{-}H3'}$ 7.9, $^{3}J_{H3'\text{-}H4'}$ 7.2, $^{4}J_{H3'\text{-}H5'}$ 1.1	2'(3), 4'(3), 5'(4)	5'(3)
4'	132.9	7.39 (ddd)	$^{3}J_{H3'\text{-}H4'}$ 7.2, $^{3}J_{H4'\text{-}H5'}$ 8.3, $^{4}J_{H2'\text{-}H4'}$ 1.7	3'(3), 5'(3), 2'(4)	3'(2), 2'(3), OH(4w)
5'	117.2	7.11 (ddd)	$^{3}J_{H4'\text{-}H5'}$ 8.3, $^{4}J_{H3'\text{-}H5'}$ 1.1, $^{5}J_{H2'\text{-}H5'}$ 0.4	4'(3), 3'(4), 2'(5w)	4'(2w), 3'(3), OH(3), 2'(4w),
6'	157.7	-	-	-	5'(2), OH(2w), 2'(3), 4'(3), 3'(4w)
OH	-	11.31 (s)	-	4'(5w)	-
$4_{triazole}$	148.8	-	-	-	$5_{triazole}$(2), 1''(2), 2''(3), 4'(3), 3(4w)
$5_{triazole}$	119.9	6.81 (s)	-	3(4w), 1''(4)	3(3), 1''(3)
1''	25.7	2.53-2.68 (m)	-	2''(3), $5_{triazole}$(4)	2''(2), 2''(2), 3''(3w), 3(5w)
2''	29.2 [d]	1.55 (quint)	$^{3}J_{H1''\text{-}H2''}$ 7.4, $^{3}J_{H2''\text{-}H3''}$ 7.4	1''(3), 3''(3)	1''(2), 3''(2)
3''	29.2 [d]	1.10-1.33 (m)	-	2''(3)	2''(2), 4''(2),
4'', 5'', 6'', 7'', 8'', 9'', 10''	29.1, 29.3, 29.46, 29.55, 29.58, 29.61, 29.64 [e,f]	1.10-1.33 (m)	-	-	-
11''	31.9	1.10-1.33 (m)	-		13''(3)
12''	22.7	1.10-1.33 (m)	-		13''(2)
13''	14.1	0.87 (t)	$^{3}J_{H12''\text{-}H13''}$ 7.0	12''(3)	12''(2)

a – m = multiplicity; *b* – n = number of chemical bonds; *c* – "w" means week intensity correlation; *d* – two resonances with identical chemical shift, as confirmed by HSQC analysis; *e* – these resonances are related to the seven indicated ^{13}C nuclei, however it was not possible to assign them unequivocally; *f* – some of the chemical shifts were indicated with two decimals in order to differentiate nuclei with very similar resonance frequencies.

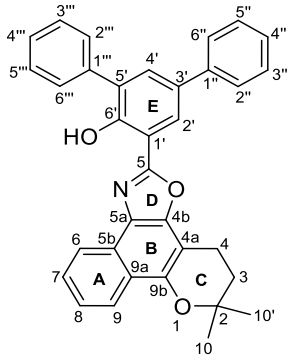

Table S3. ^{1}H and ^{13}C NMR data of **P3** in $CDCl_3$ at 303 K

(^{1}H and ^{13}C data recorded at 400 and 100 MHz, respectively)

Index	δ ^{13}C/ppm	δ ^{1}H (m)/ppm [a]	^{n}J/Hz [b]	COSY (n)[b,c]	HMBC (n)[b,c]
2	75.5	-	-	-	3(2), 10/10'(2), 4(3)
3	31.7	2.01 (t)	$^{3}J_{H3\text{-}H4}$ 6.6	4(3)	4(2), 10/10'(3)
4	17.5	3.14 (t)	$^{3}J_{H3\text{-}H4}$ 6.6	3(3)	3(2), 10/10'(4w)
5	160.4	-	-	-	2'(3)
6	121.6	8.30 (dd)	$^{3}J_{H6\text{-}H7}$ 8.3, $^{4}J_{H6\text{-}H8}$ 1.1	7(3)	8(3)
7	127.1[e]	7.60 (ddd)	$^{3}J_{H6\text{-}H7}$ 6.9, $^{3}J_{H7\text{-}H8}$ 8.3, $^{4}J_{H5\text{-}H7}$ 1.2	6(3), 8(3)	9(3)
8	124.9	7.44-7.53 (m)	-	7(3), 9(3)	6(3)
9	122.8	8.30 (dd)	$^{3}J_{H8\text{-}H9}$ 8.3, , $^{4}J_{H7\text{-}H9}$ 1.1	8(3)	7(3)
10/10'	26.8	1.49 (s)	-		3(3), 10'/3(3), 10(3)
4a	101.7	-	-	-	4(2), 3(3)
4b	146.5	-	-	-	4(3)
5a	127.5	-	-	-	6(3), 4(4,w)
5b	124.4	-	-	-	7(3), 9(3)
9a	124.2	-	-	-	6(3), 8(3), 4(4w)
9b	148.4	-	-	-	4(3), 9(3)
1'	112.1	-	-	-	4'(4w)
2'	123.8	8.23 (d)	$^{4}J_{H2'\text{-}H4'}$ 2.4	4'(4)	4'(3)
3'	140.4	-	-	-	2'(2), 4'(2), 3''(4), 5''(4)
4'	132.1	7.70 (d)	$^{4}J_{H2'\text{-}H4'}$ 2.4	2'(4)	2'(3)
5'	137.9	-	-	-	4'(2), 3'''(4), 5'''(4)
6'	154.4	-	-	-	2'(3), 4'(3)
OH	-	12.20 (s)	-		-
1''	132.7	-	-	-	2''(2), 6''(2)
2''/6''	126.9	7.66-7.69 (m)	-	3''(3)/5''(3)	3''(2), 6''(3), 4''(3)/5''(w), 2''(3), 4''(3)
3''/5''	128.9	7.44-7.53 (m)	-	2''(3)/6''(3)	2''(2w); 5''(3) / 4''(2w); 3''(3)
4''	127.1 [e]	-	-	-	2''(3), 6''(3),
1'''	130.6	-	-	-	2'''(2), 6'''(2)
2'''/6'''	129.5	7.72-7.76 (m)	-	3'''(3)/5'''(3)	3'''(2), 6'''(3), 4'''(3)/5'''(w), 2'''(3), 4'''(3)
3'''/5'''	128.2	7.44-7.53 (m)	-	2'''(3)/6'''(3)	2'''(2w); 5'''(3) / 4'''(2w); 3'''(3)
4'''	127.4	-	-	-	2'''(3),6'''(3)

a – m = multiplicity; *b* – n = number of chemical bonds; *c* – "w" means week intensity correlation; *d* – two resonances with identical chemical shift, as confirmed by HSQC analysis.

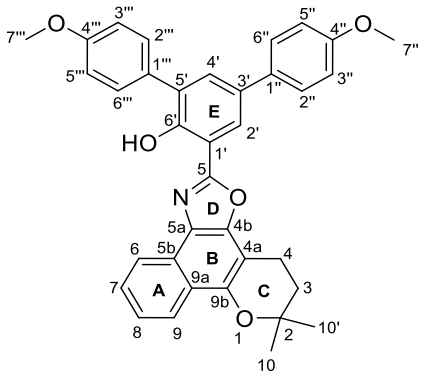

Table S4. ^{1}H and ^{13}C NMR data of **P4** in $CDCl_3$ at 303 K

(^{1}H and ^{13}C data recorded at 400 and 100 MHz, respectively)

Index	δ ^{13}C/ppm	δ ^{1}H (m)/ppm [a]	^{n}J/Hz [b]	COSY (n)[b,c]	HMBC (n)[b,c]
2	75.5	-	-	-	3(2), 10/10'(2), 4(3)
3	31.7	2.00 (t)	$^{3}J_{H3\text{-}H4}$ 6.4	4(3)	4(2), 10/10'(3)
4	17.5	3.13 (t)	$^{3}J_{H3\text{-}H4}$ 6.4	3(3)	3(2), 10/10'(4)
5	160.6	-	-	-	2'(3)
6	121.6	8.28 (d)	$^{3}J_{H6\text{-}H7}$ 8.6	7(3)	8(3)
7	127.0	7.55-7.63 (m)	-	6(3), 8(3)	9(3)
8	124.8	7.44-7.52 (m)	-	7(3), 9(3)	6(3)
9	122.8	8.28 (d)	$^{3}J_{H8\text{-}H9}$ 8.6	8(3)	7(3)
10/10'	26.8	1.48 (s)	-		3(3), 10'/3(3), 10(3)
4a	101.7	-	-	-	4(2), 3(3)
4b	146.4	-	-	-	4(3)
5a	127.5	-	-	-	6(3), 4(4,w)
5b	124.4	-	-	-	7(3), 9(3)
9a	124.1	-	-	-	6(3), 8(3), 4(4w)
9b	148.3	-	-	-	4(3), 9(3)
1'	111.9	-	-	-	4'(4w)
2'	122.9	8.12 (d)	$^{4}J_{H2'\text{-}H4'}$ 1.8	4'(4)	4'(3)
3'	133.1	-	-	-	2'(2), 4'(2), 3''(4), 5''(4)
4'	131.6	7.55-7.63 (m)	-	2'(4)	2'(3)
5'	130.3	-	-	-	4'(2), 3'''(4), 5'''(4)
6'	153.9	-	-	-	2'(3), 4'(3)
OH	-	12.11 (s)	-		-
1''	132.4	-	-	-	2''(2), 6''(2)
2''/6''	127.9	7.55-7.63 (m)	-	3''(3)/5''(3)	3''(2w), 6''(3) / 5''(2w),2''(3)
3''/5''	114.3	6.99 (d)	$^{3}J_{H2''\text{-}H3''}$ 8.7/$^{3}J_{H5''\text{-}H6''}$ 8.7	2''(3)/6''(3)	2''(2); 5''(3) / 4''(2); 3''(3)
4''	159.0	-	-	-	3''(2w), 5''(2w), 2''(3), 6''(3), 7''(3)
7''	55.4	3.85 (s)	-		
1'''	130.1	-	-	-	2'''(2), 6'''(2), 3'''(3), 5'''(3)
2'''/6'''	130.6	7.67 (d)	$^{3}J_{H2'''\text{-}H3'''}$ 8.4 / $^{3}J_{H5'''\text{-}H6'''}$ 8.4	3'''(3)/5'''(3)	6'''(3)/2'''(3)
3'''/5'''	113.7	7.03 (d)	$^{3}J_{H2'''\text{-}H3'''}$ 8.4 / $^{3}J_{H5'''\text{-}H6'''}$ 8.4	2'''(3)/6'''(3)	2'''(2); 5'''(3); / 4'''(2); 3'''(3)
4'''	159.1	-	-	-	3'''(2w),5'''(2w), 2'''(3),6'''(3), 7'''(3)
7'''	55.4	3.87 (s)	-		

a – m = multiplicity; *b* – n = number of chemical bonds; *c* – "w" means week intensity correlation.

NMR spectra

Compound 2 (nor-lapachol)

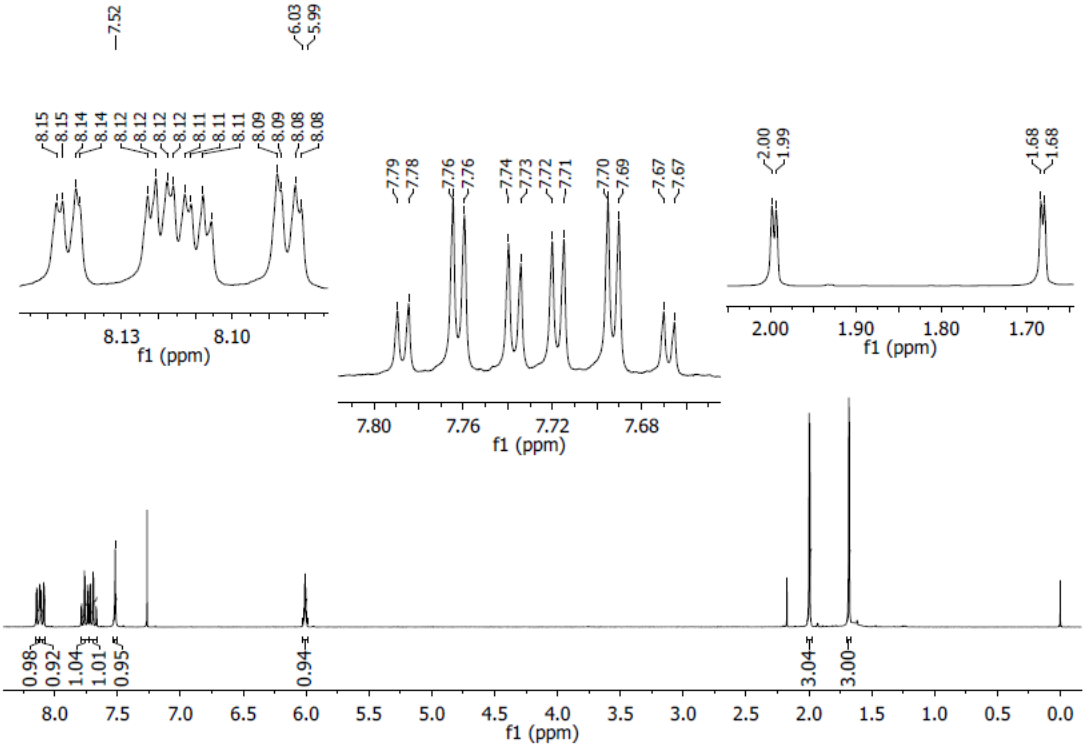

Figure S1. ^{1}H NMR spectrum of compound **2** at 400 MHz in $CDCl_3$ (303 K).

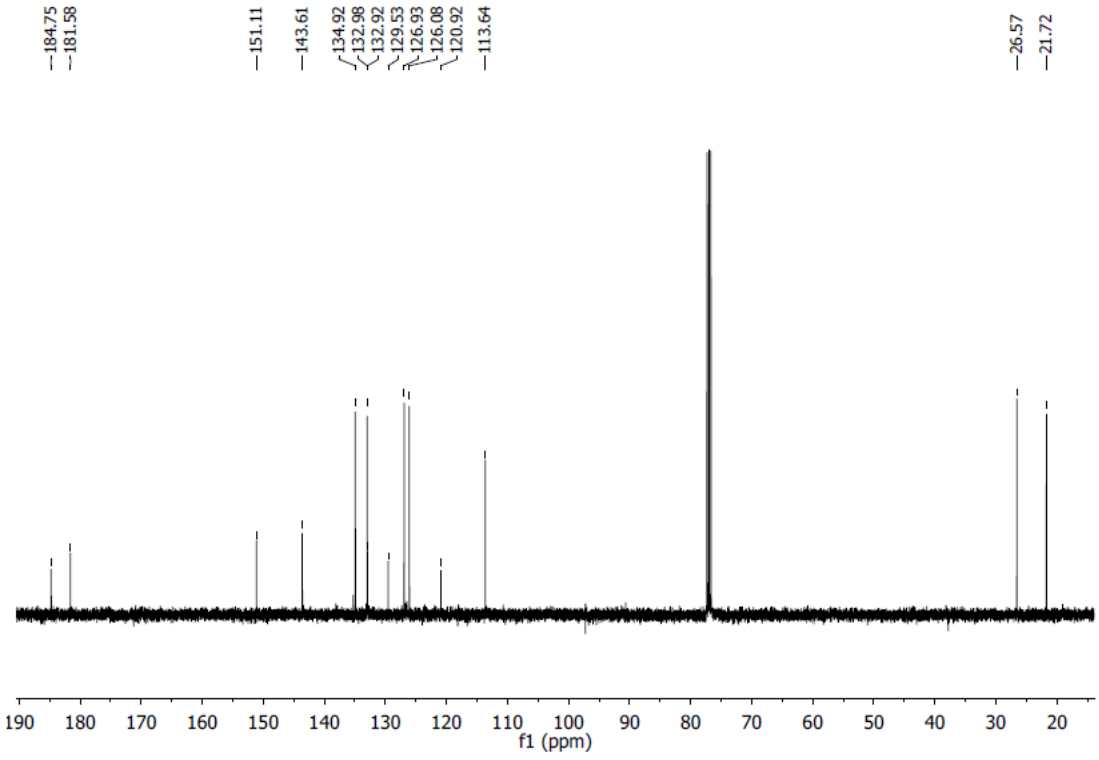

Figure S2. ^{13}C NMR spectrum of compound **2** at 100 MHz in $CDCl_3$ (303 K).

Compound 3

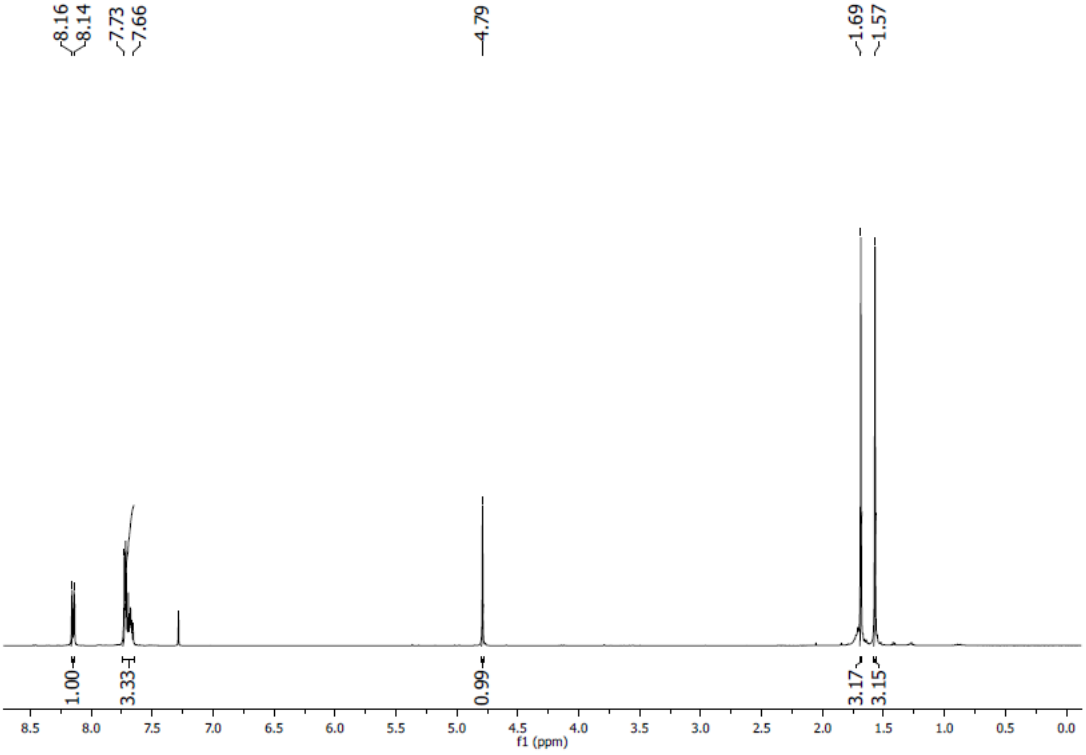

Figure S3. ^{1}H NMR spectrum of compound **3** at 400 MHz in $CDCl_3$ (303 K).

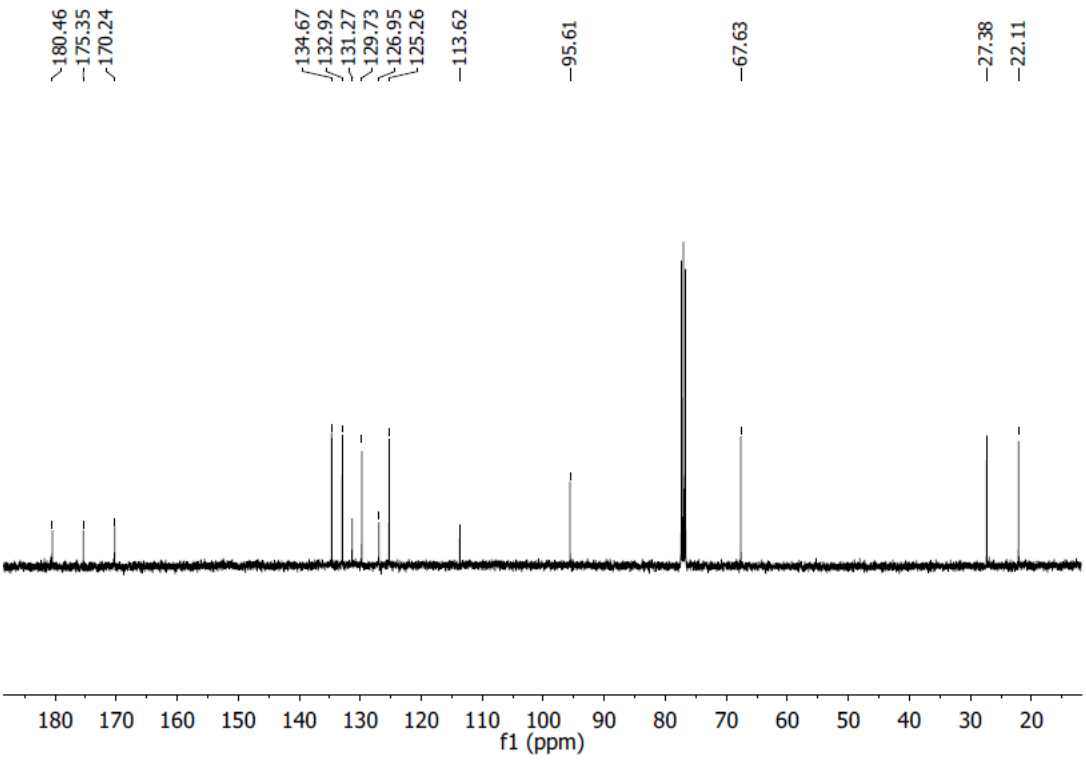

Figure S4. ^{13}C NMR spectrum of compound **3** at 100 MHz in $CDCl_3$ (303 K).

Compound 4 (β-lapachone)

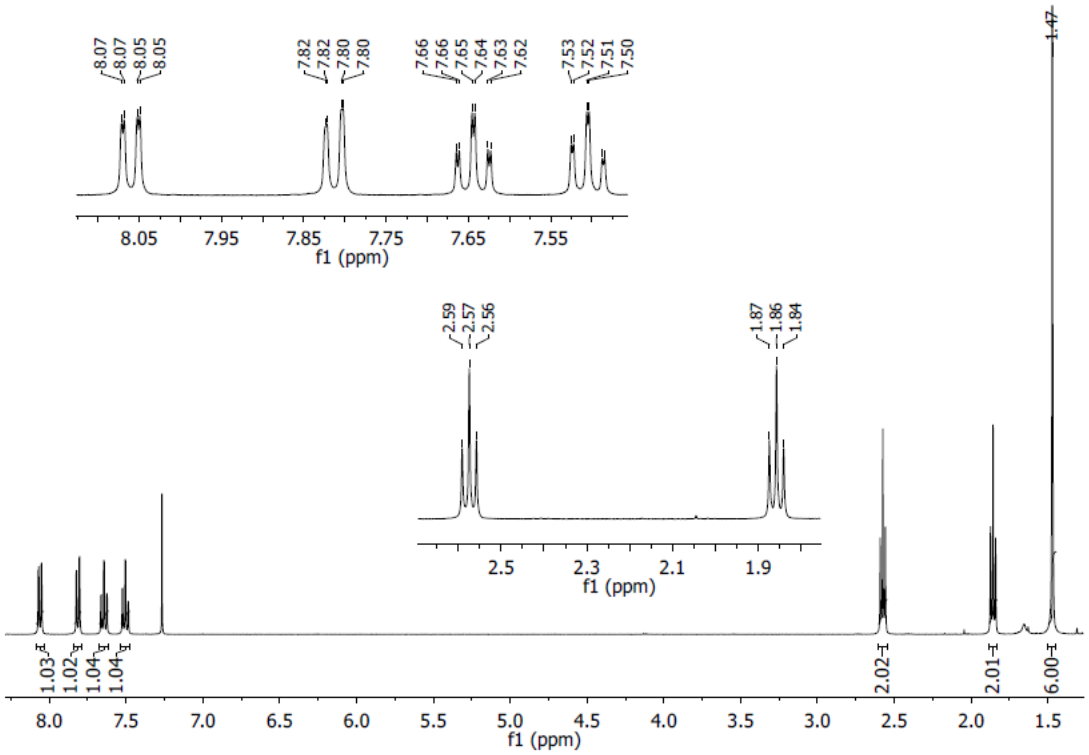

Figure S5. ^{1}H NMR spectrum of compound **4** at 400 MHz in $CDCl_3$ (303 K).

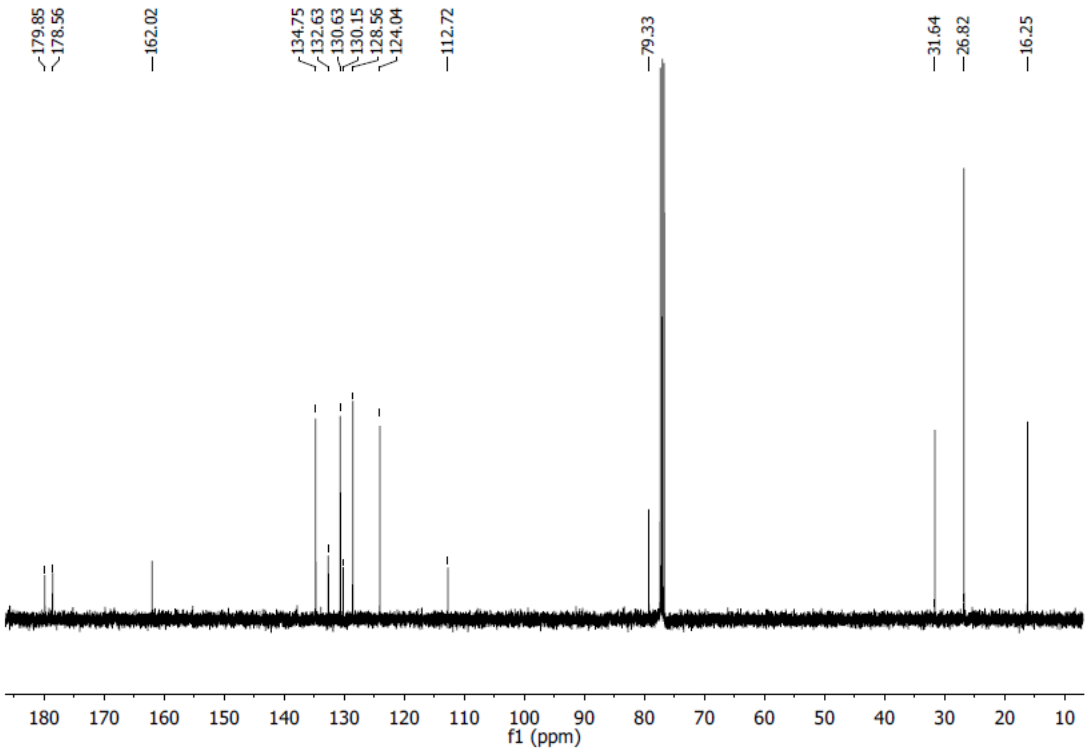

Figure S6. ^{13}C NMR spectrum of compound **4** at 100 MHz in $CDCl_3$ (303 K).

Iodinated Oxazole (Compound 5)

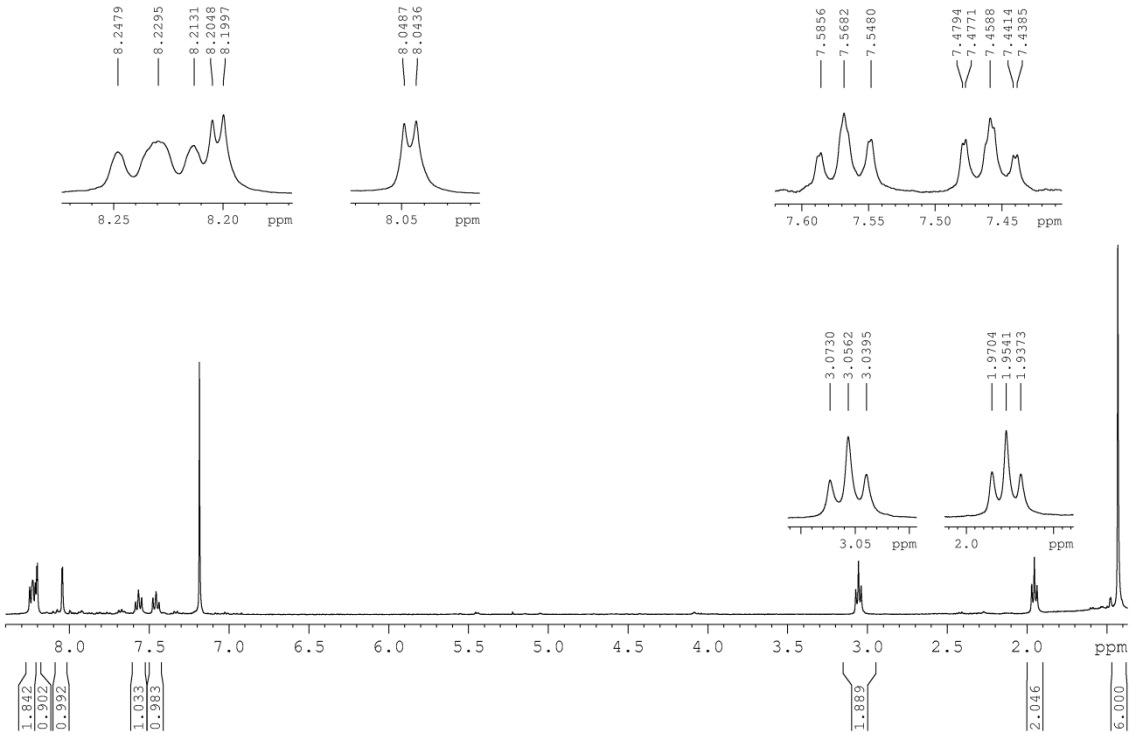

Figure S7. ^{1}H NMR spectrum of compound **5** at 400 MHz in $CDCl_3$ (303 K).

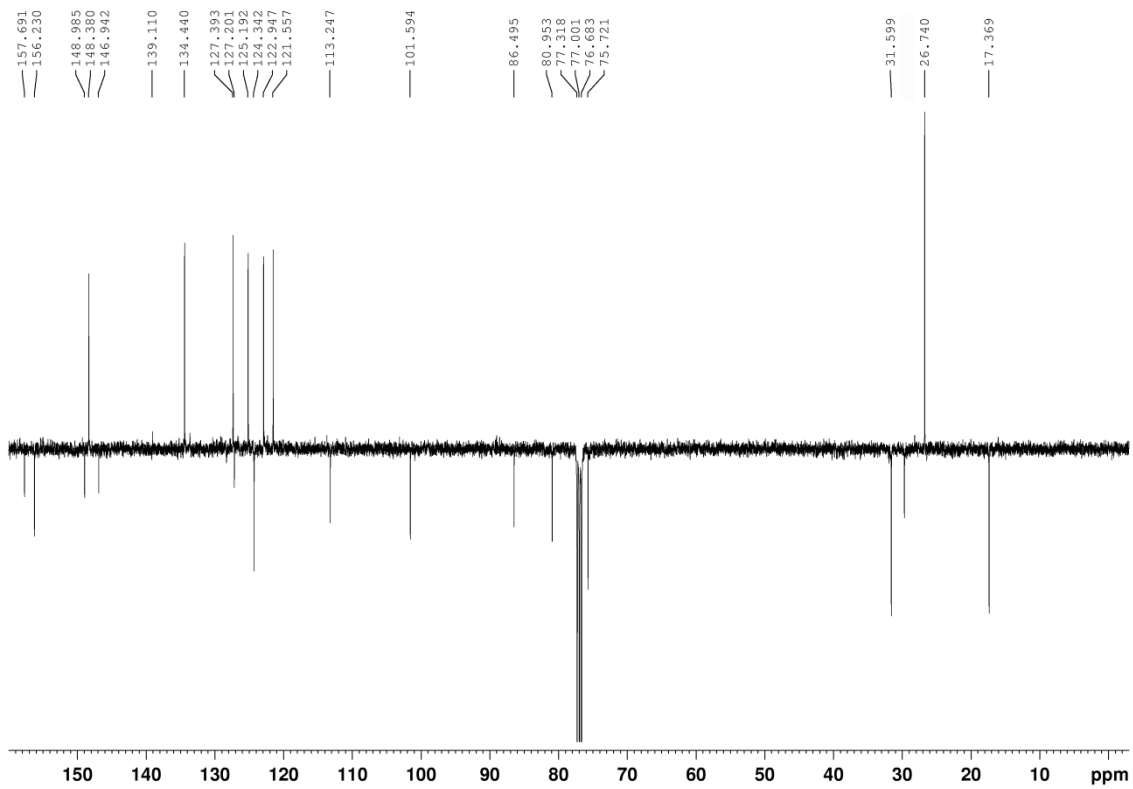

Figure S8. APT spectrum of compound **5** at 100 MHz in $CDCl_3$ (303 K).

Compound P1

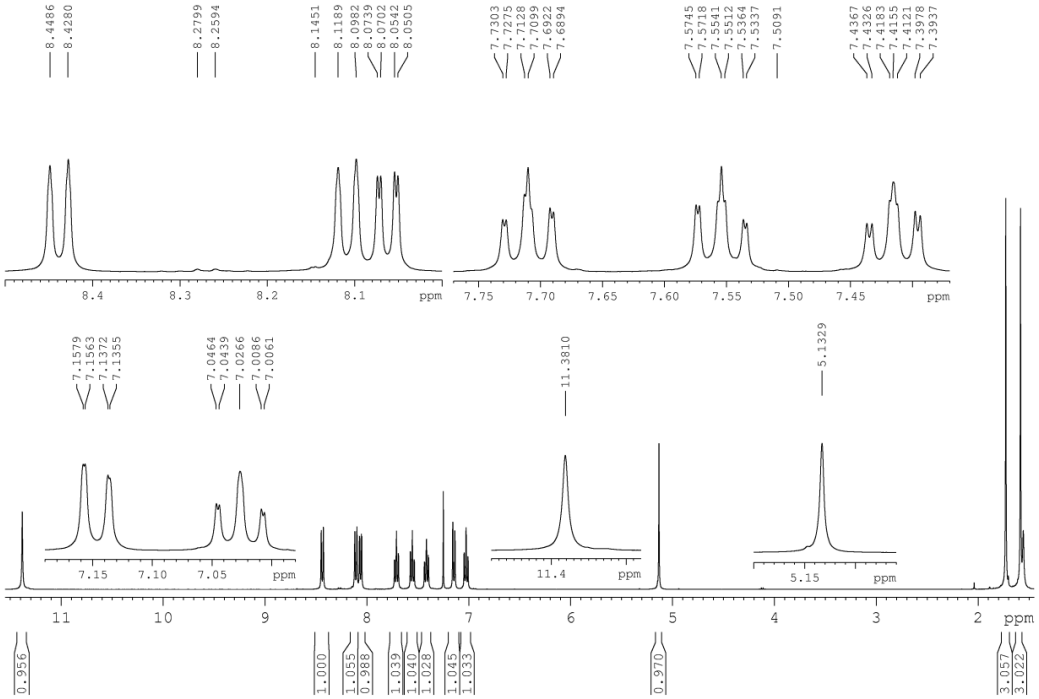

Figure S9. ^{1}H NMR spectrum of **P1** at 400 MHz in $CDCl_3$ (303 K).

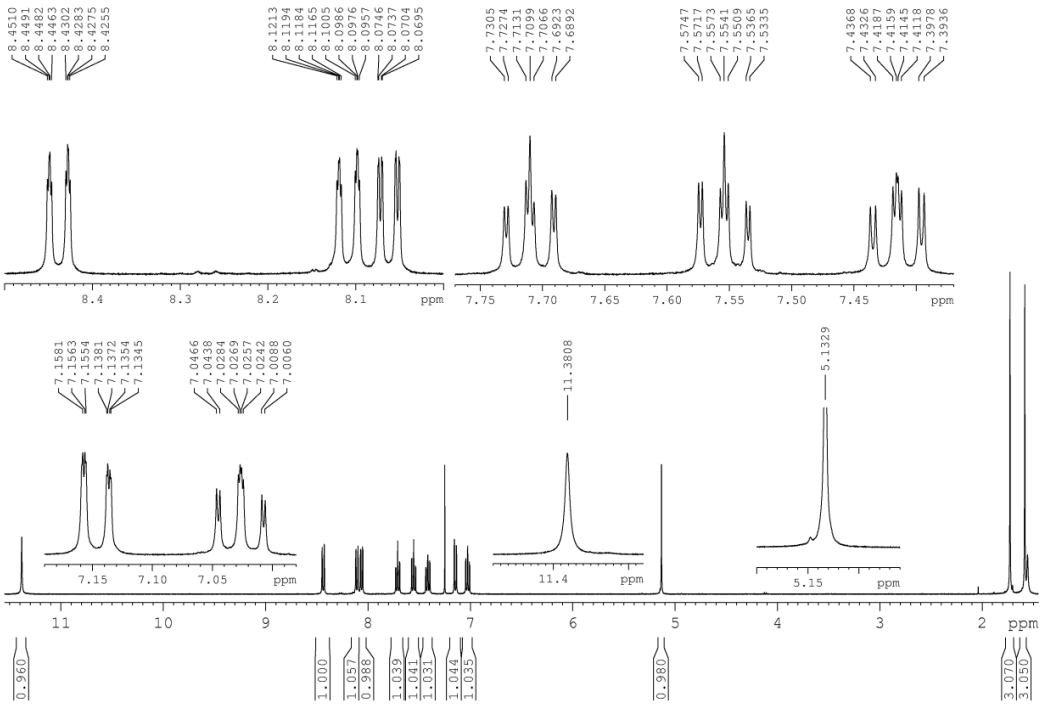

Figure S10. ^{1}H NMR spectrum of **P1** at 400 MHz in $CDCl_3$ (303 K). Lorentz-Gauss transformation (lb = -0.3, gb = 40 %).

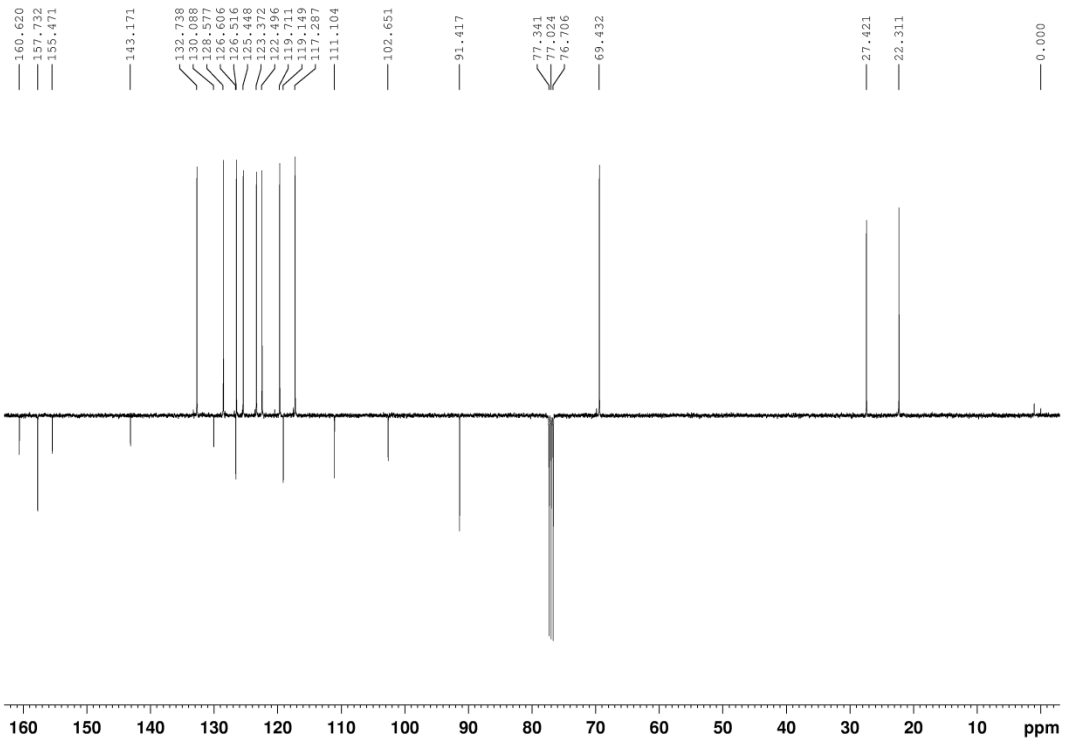

Figure S11. APT spectrum of **P1** at 100 MHz in $CDCl_3$ (303 K).

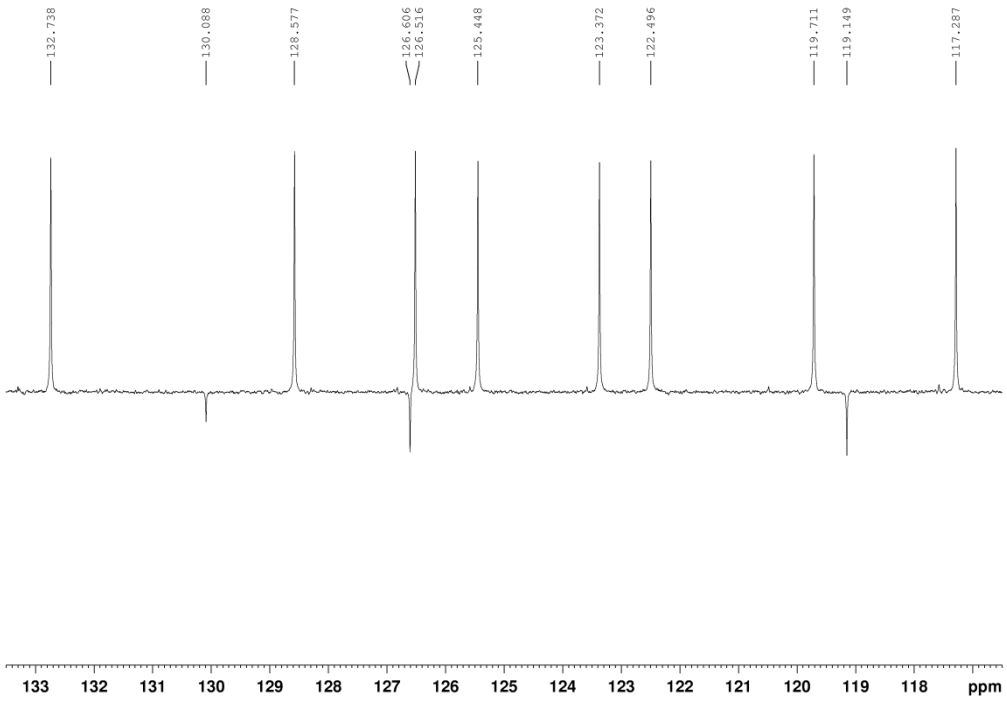

Figure S12. Expanded APT spectrum of **P1** at 100 MHz in $CDCl_3$ (303 K).

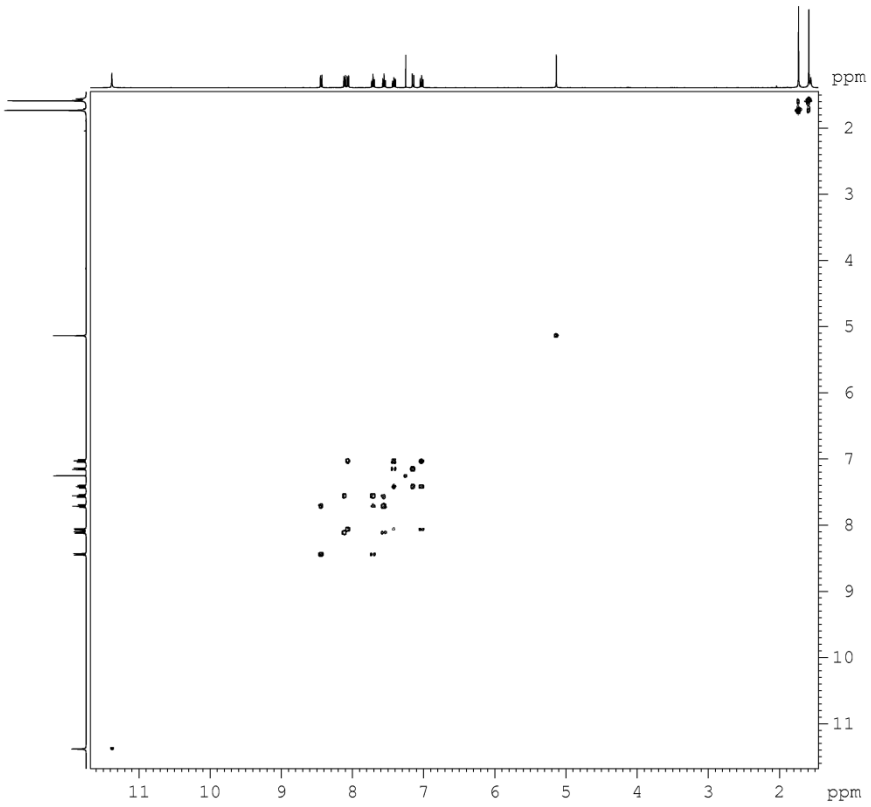

Figure S13. COSY spectrum of **P1** at 400 MHz in $CDCl_3$ (303 K).

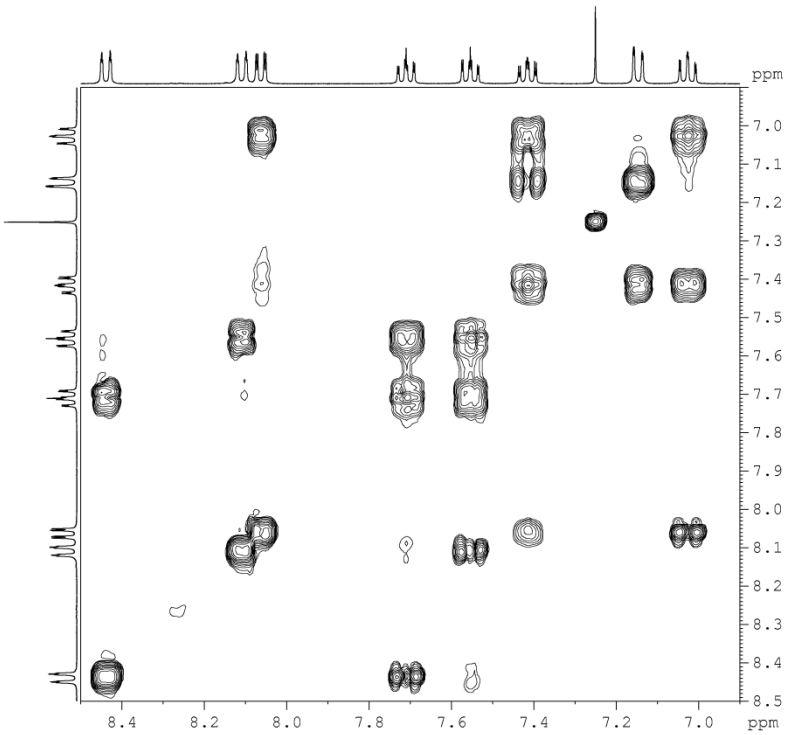

Figure S14. Expanded COSY spectrum of **P1** at 400 MHz in $CDCl_3$ (303 K) showing the correlations between aromatic ^1H resonances.

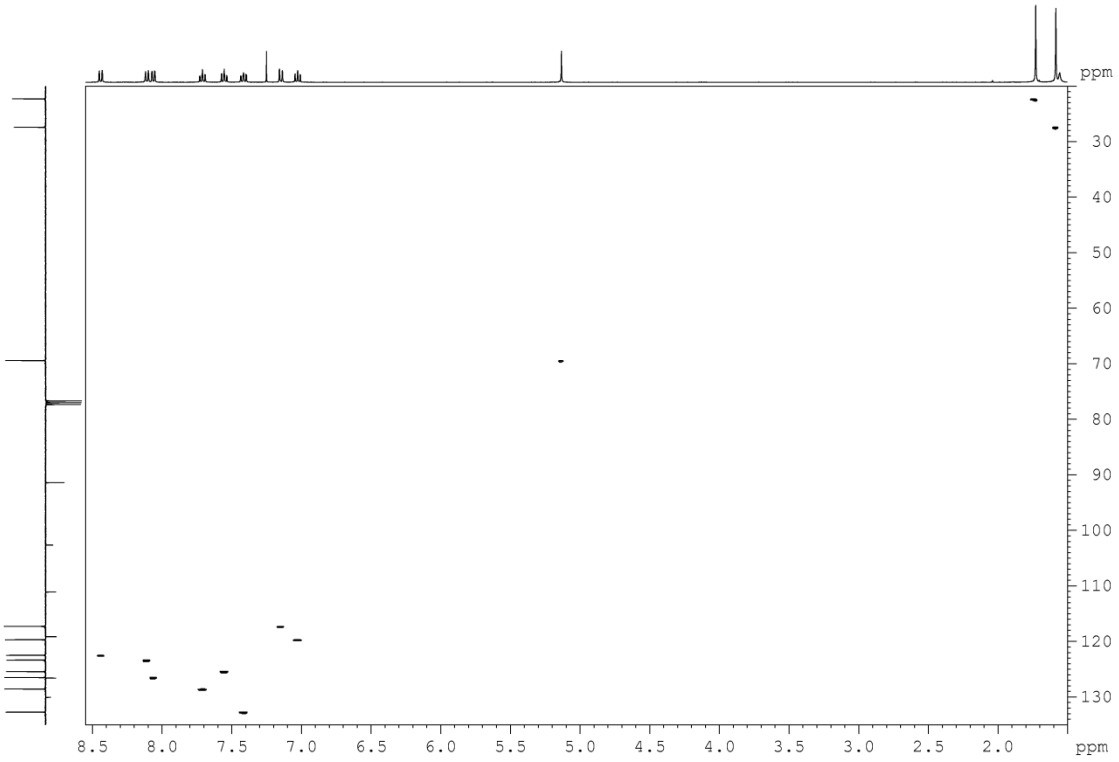

Figure S15. ^{1}H-^{13}C HSQC spectrum of **P1** at 400 MHz in $CDCl_3$ (303 K).

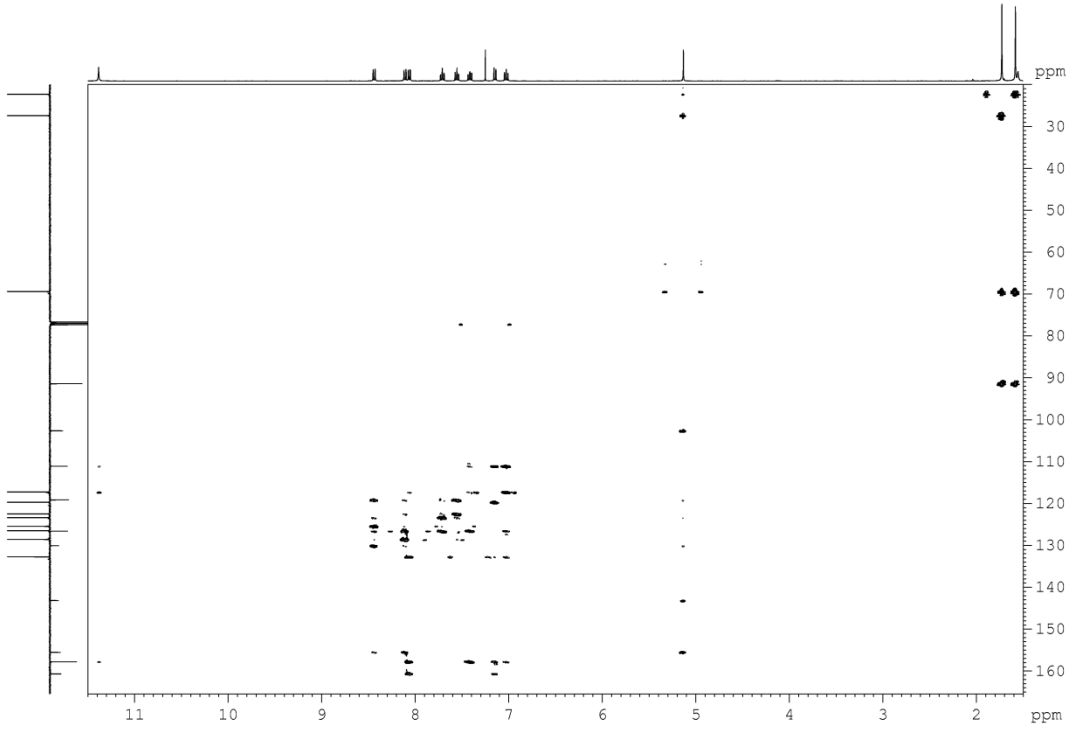

Figure S16. ^{1}H-^{13}C HMBC spectrum of **P1** at 400 MHz in $CDCl_3$ (303 K).

Compound P2

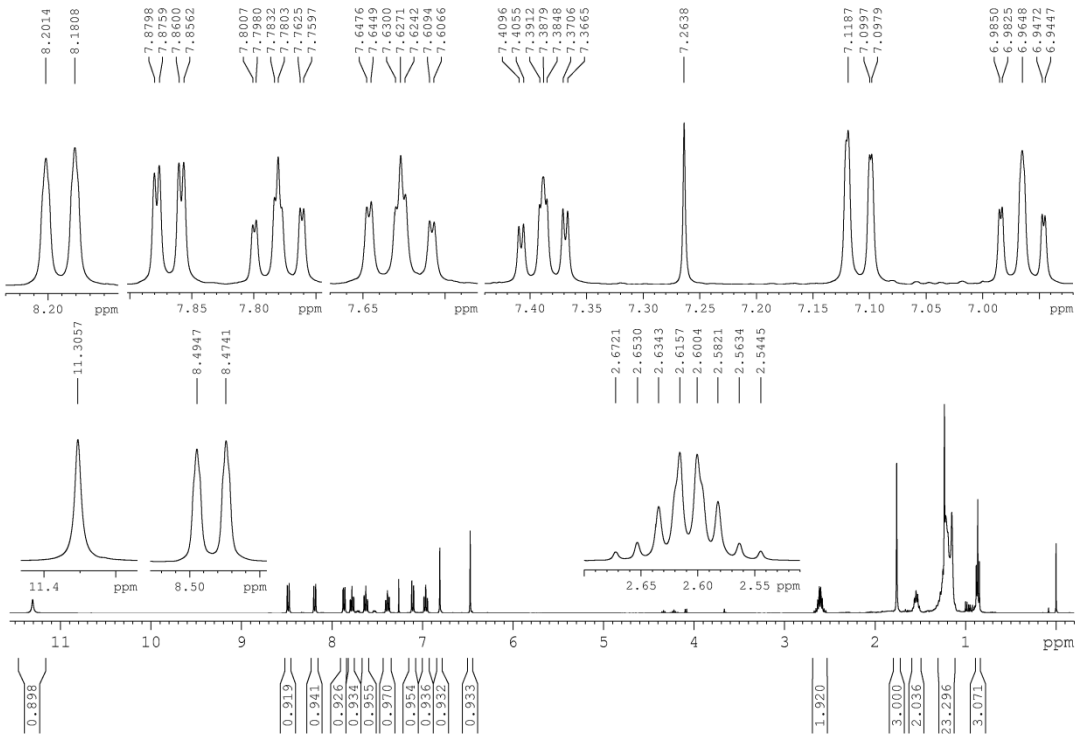

Figure S17. [1]HNMR spectrum of **P2** at 400 MHz in $CDCl_3$ (303 K).

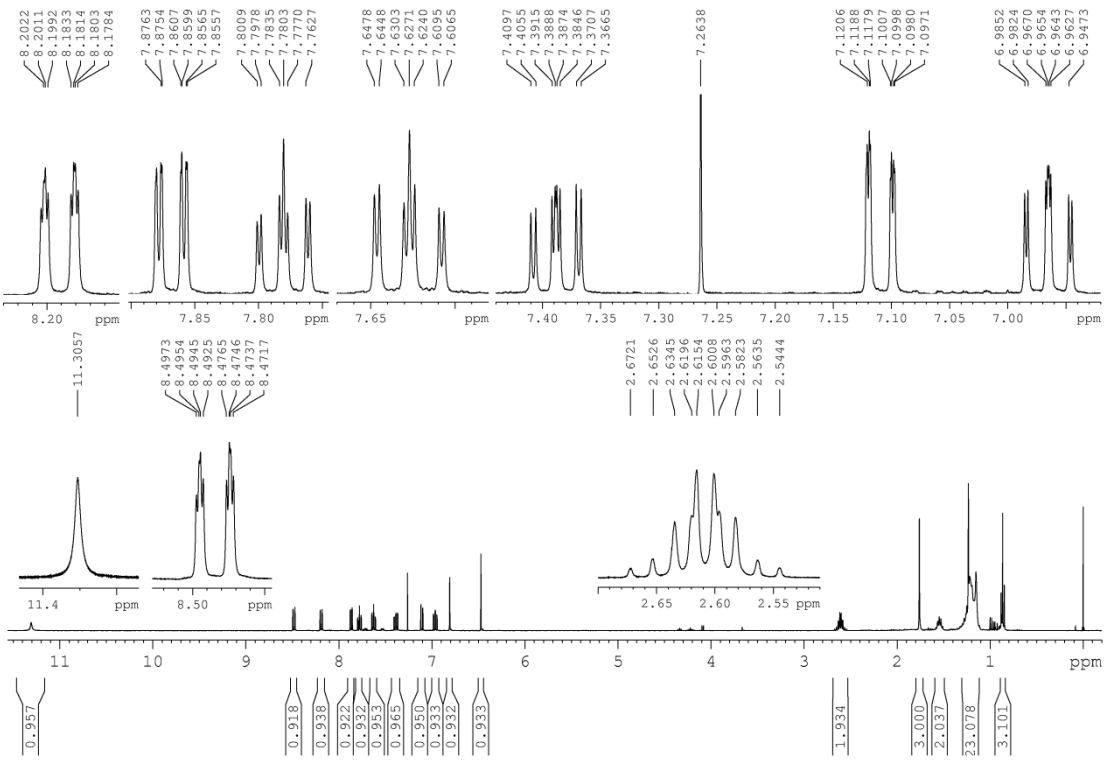

Figure S18.[1]H NMR spectrum of **P2** at 400 MHz in $CDCl_3$ (303 K).Lorentz-Gauss transformation (lb = -0.4, gb =50 %).

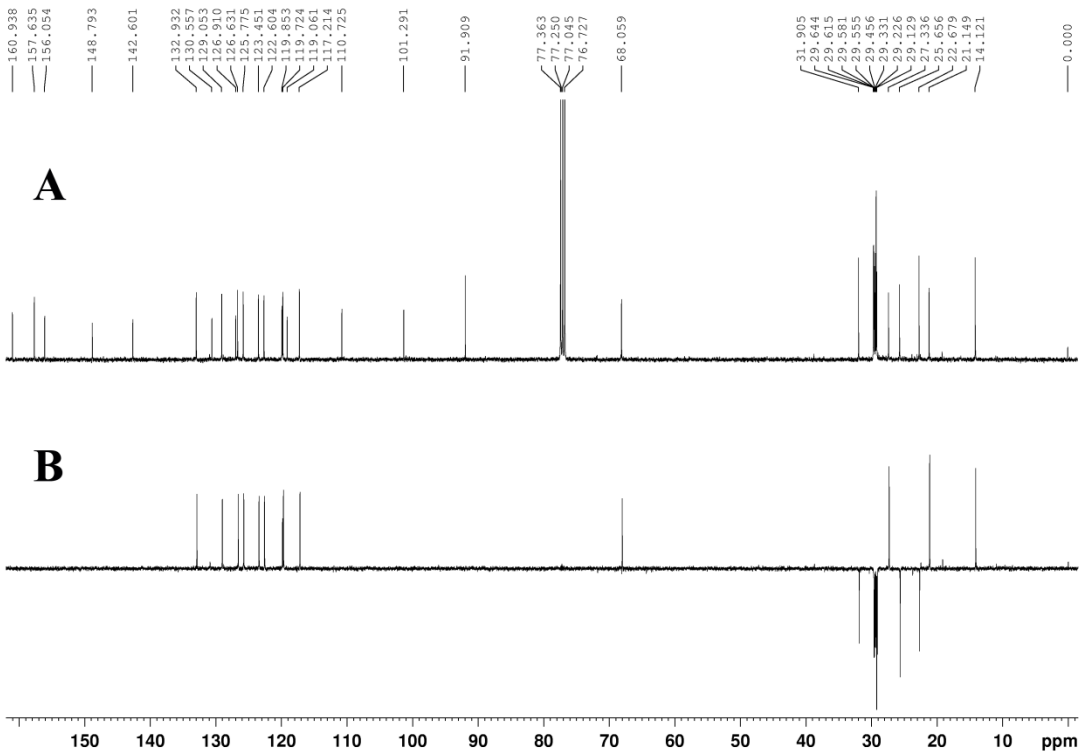

Figure S19. (A) ^{13}C NMR and (B) DEPT-135 spectra of **P2** at 100 MHz in $CDCl_3$ (303 K).

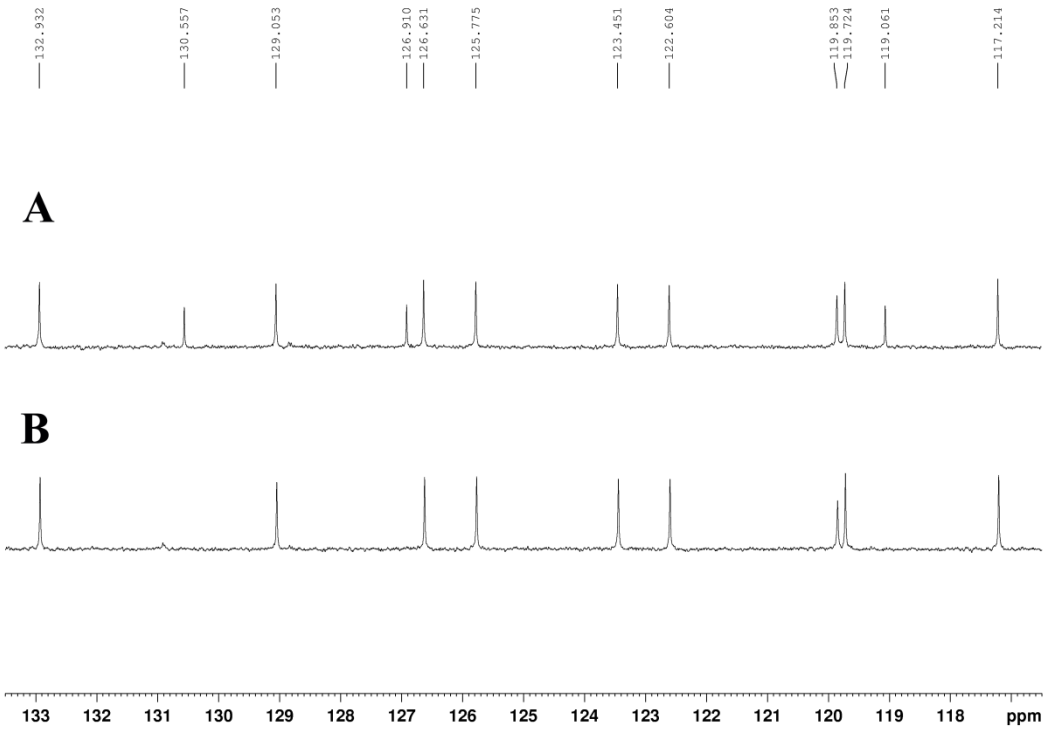

Figure S20. Expanded (A) ^{13}C NMR and (B) DEPT-135 spectra of **P2** at 100 MHz in $CDCl_3$ (303 K).

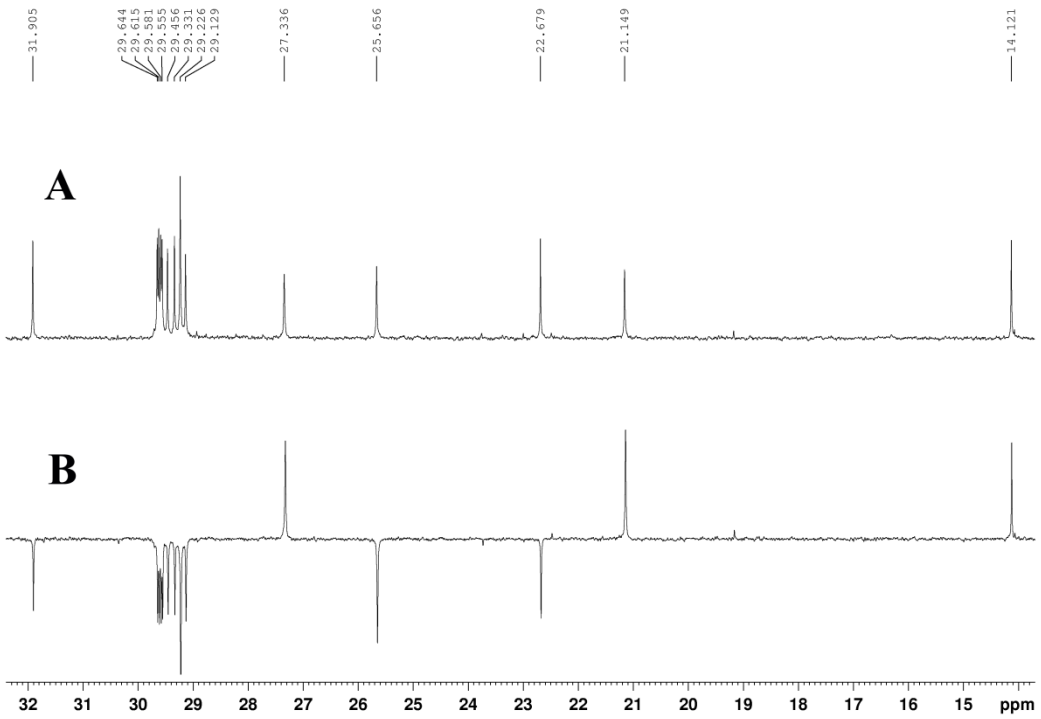

Figure S21. Expanded (A) ^{13}C NMR and (B) DEPT-135 spectra of **P2** at 100 MHz in $CDCl_3$ (303 K).

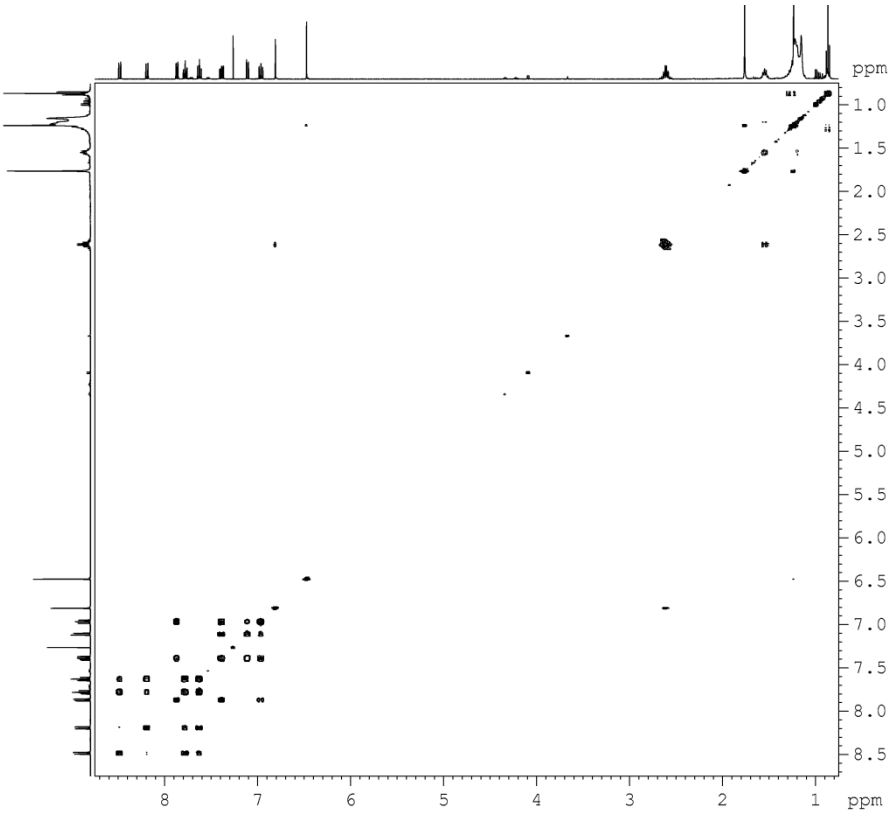

Figure S22. COSY spectrum of **P2** at 400 MHz in $CDCl_3$ (303 K) showing the correlations between aromatic ^1H resonances.

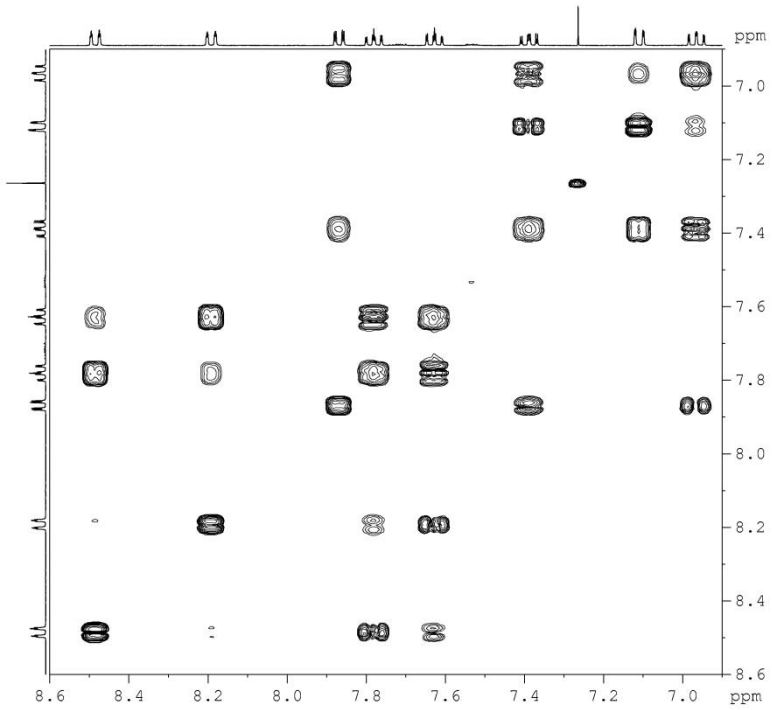

Figure S23. Expanded COSY spectrum of **P2** at 400 MHz in $CDCl_3$ (303 K) showing the correlations between aromatic ^1H resonances.

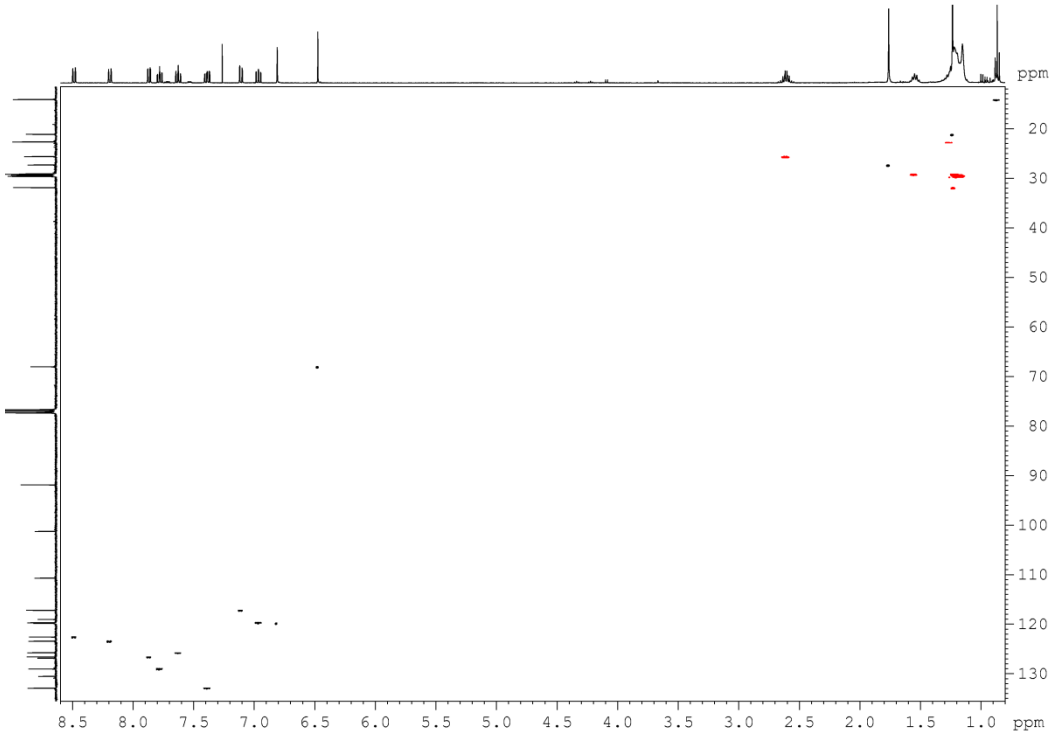

Figure S24. ^1H-^{13}C HSQC spectrum of **P2** at 400 MHz in $CDCl_3$ (303 K). Correlations in black represent peaks with positive phase (CH_3 and CH correlations) whereas the correlation in red indicates negative intensities (CH_2 correlations).

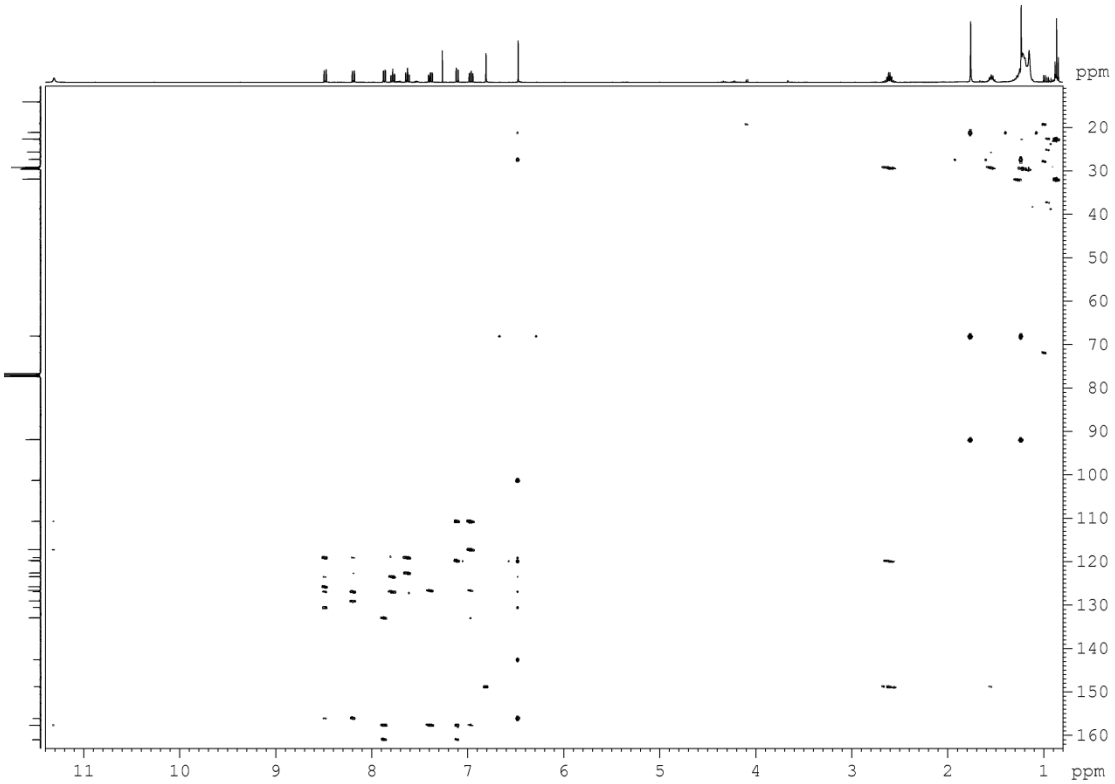

Figure S25. ^{1}H-^{13}C HMBC spectrum of **P2** at 400 MHz in $CDCl_3$ (303 K).

Compound P3

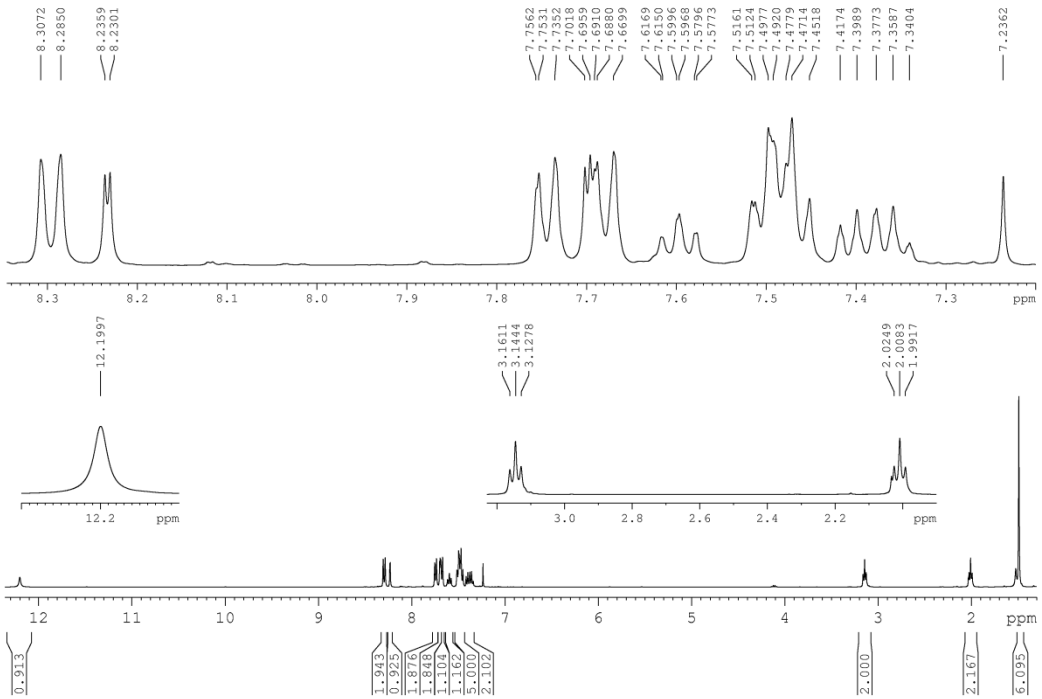

Figure S26. ^{1}H NMR spectrum of **P3** at 400 MHz in $CDCl_3$ (303 K).

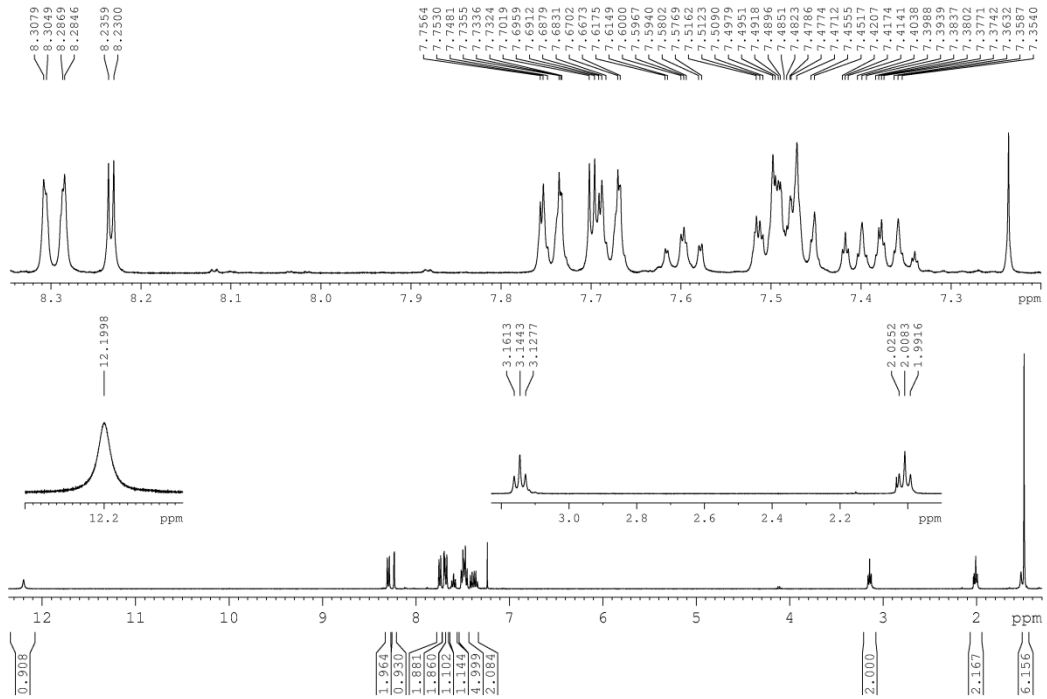

Figure S27. ^{1}H NMR spectrum of **P3** at 400 MHz in $CDCl_3$ (303 K).Lorentz-Gauss transformation (lb = -0.5, gb = 50 %).

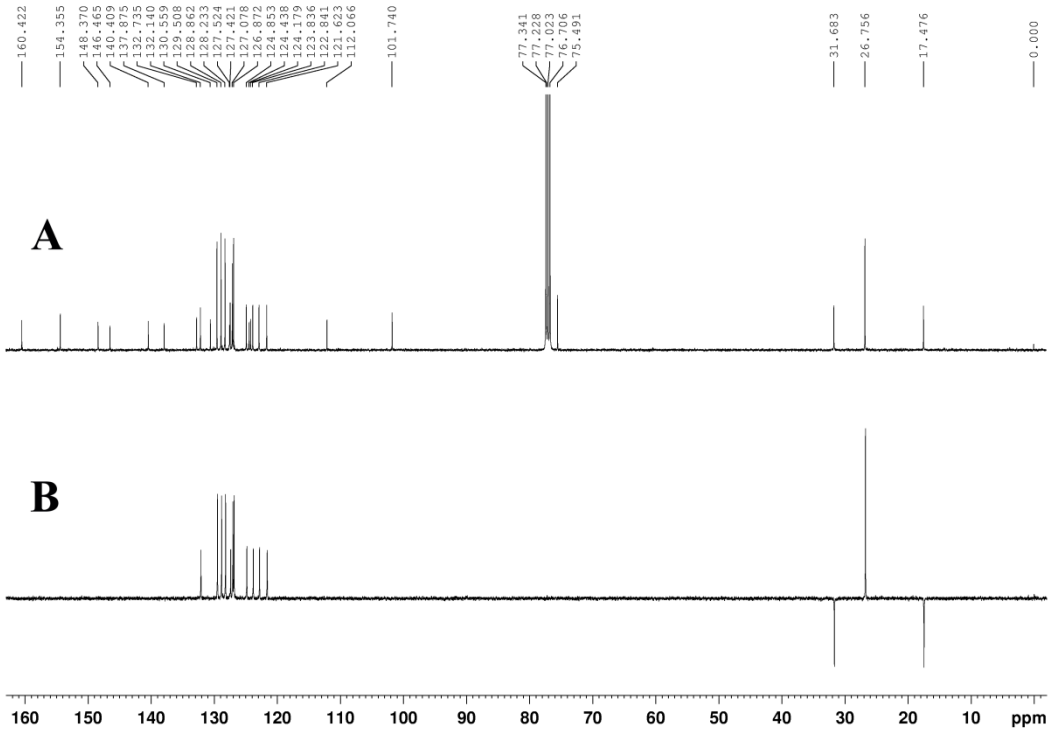

Figure S28. (A) ^{13}C NMR and (B) DEPT-135 spectra of **P3** at 100 MHz in $CDCl_3$ (303 K).

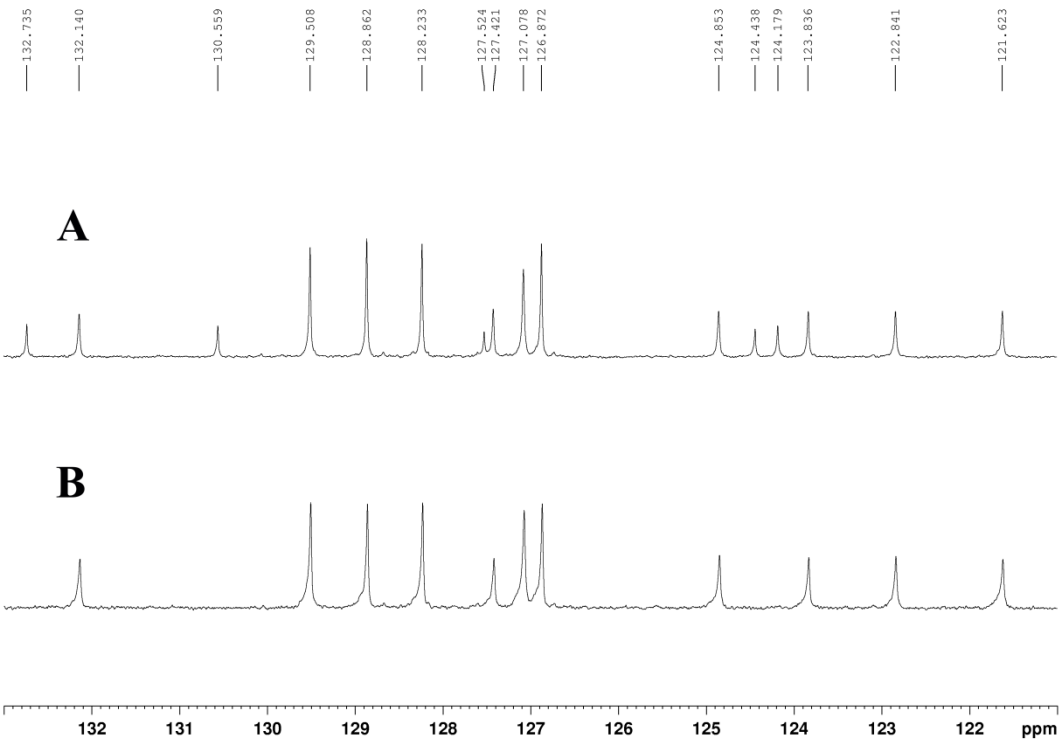

Figure S29. Expanded (A) ^{13}C NMR and (B) DEPT-135 spectra of **P3** at 100 MHz in $CDCl_3$ (303 K).

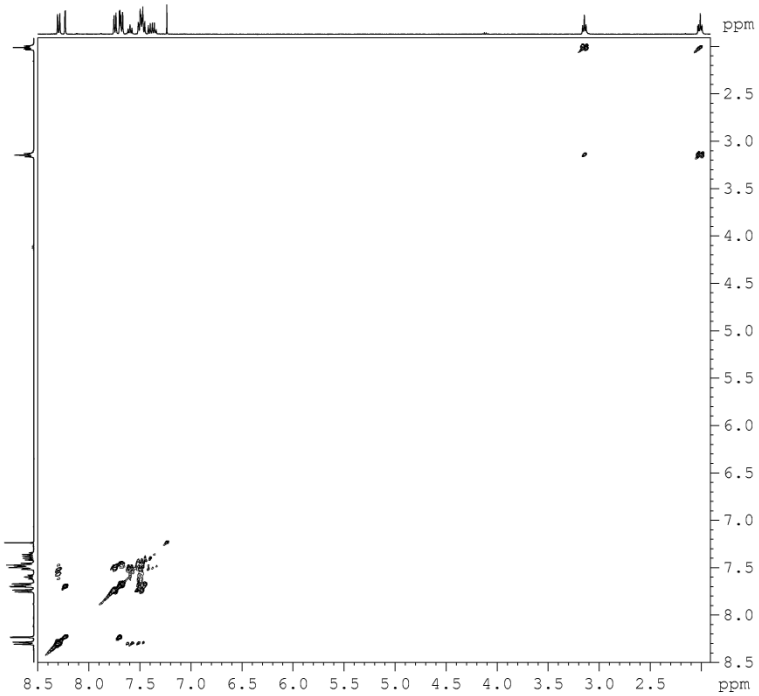

Figure S30. COSY spectrum of **P3** at 400 MHz in $CDCl_3$ (303 K).

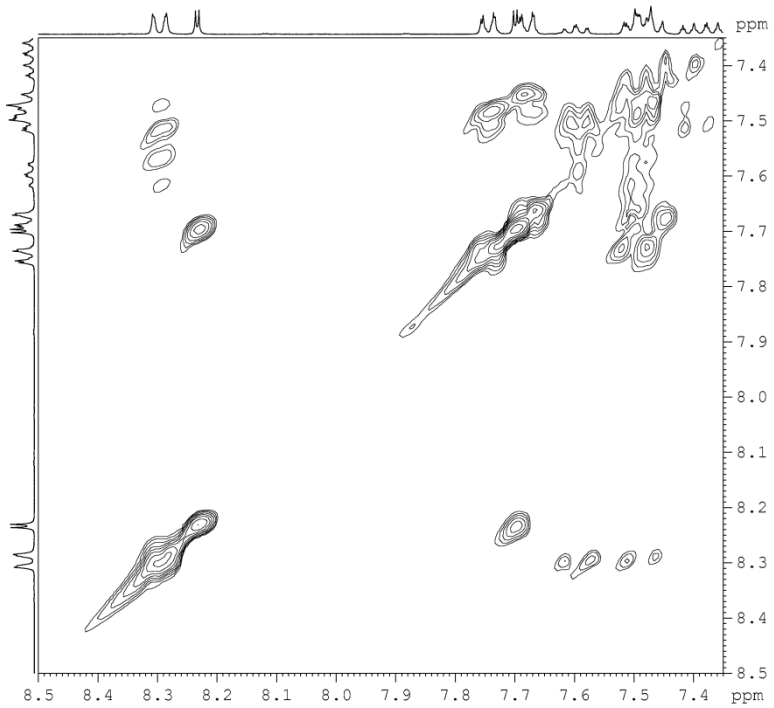

Figure S31. Expanded COSY spectrum of **P3** at 400 MHz in $CDCl_3$ (303 K) showing the correlations between aromatic ^1H resonances.

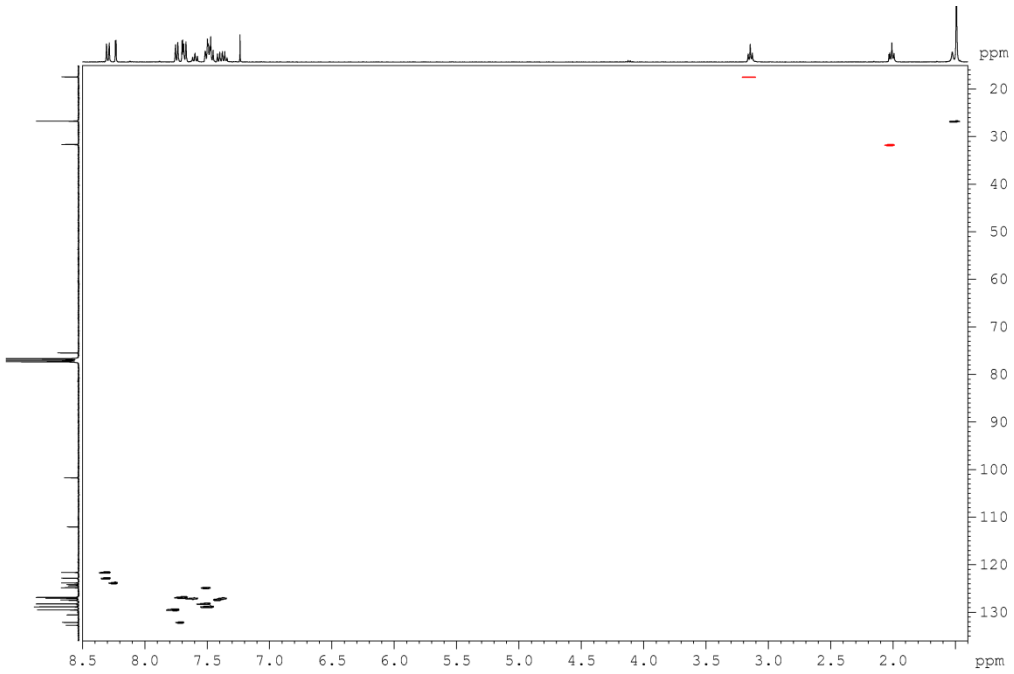

Figure S32. ^1H-^{13}C HSQC spectrum of **P3** at 400 MHz in $CDCl_3$ (303 K). Correlations in black represent peaks with positive phase (CH_3 and CH correlations) whereas the correlation in red indicates negative intensities (CH_2 correlations).

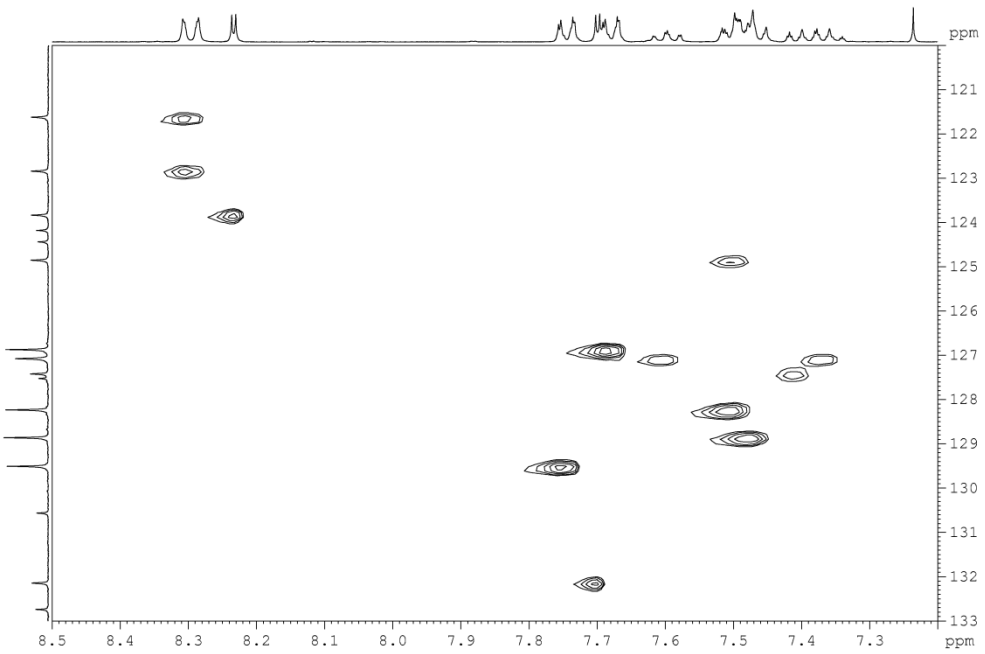

Figure S33. Expanded ^{1}H-^{13}C HSQC spectrum of **P3** at 400 MHz in $CDCl_3$ (303 K). Correlations in black represent peaks with positive phase (CH_3 and CH correlations) whereas the correlation in red indicates negative intensities (CH_2 correlations).

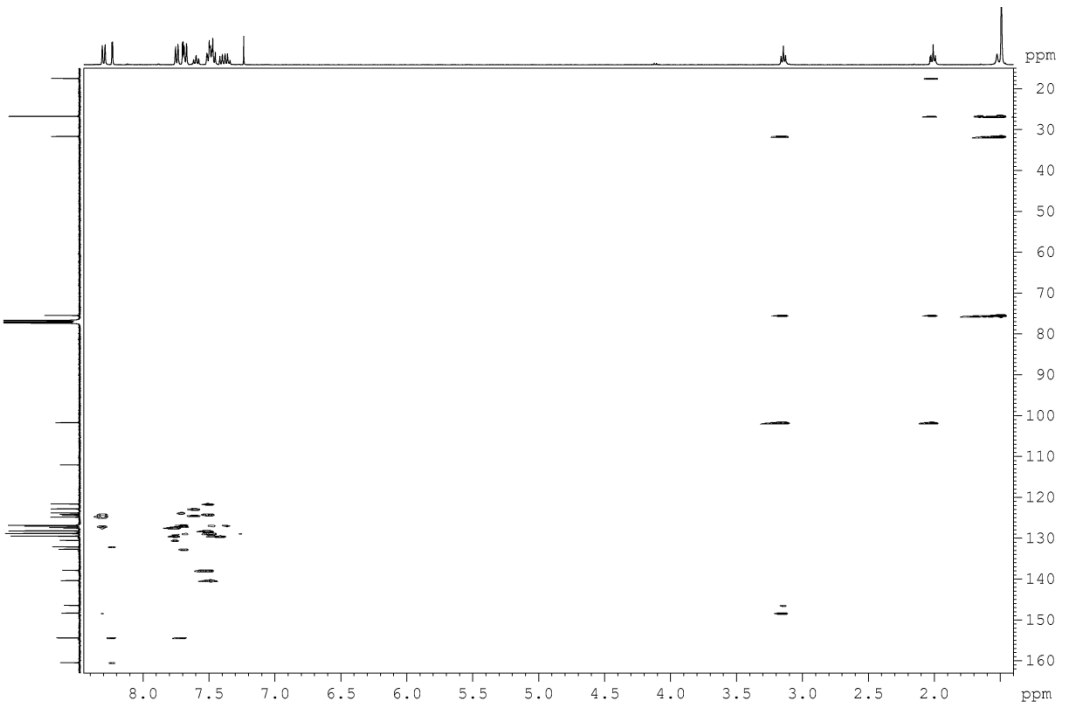

Figure S34. ^{1}H-^{13}C HMBC spectrum of **P3** at 400 MHz in $CDCl_3$ (303 K).

Compound P4

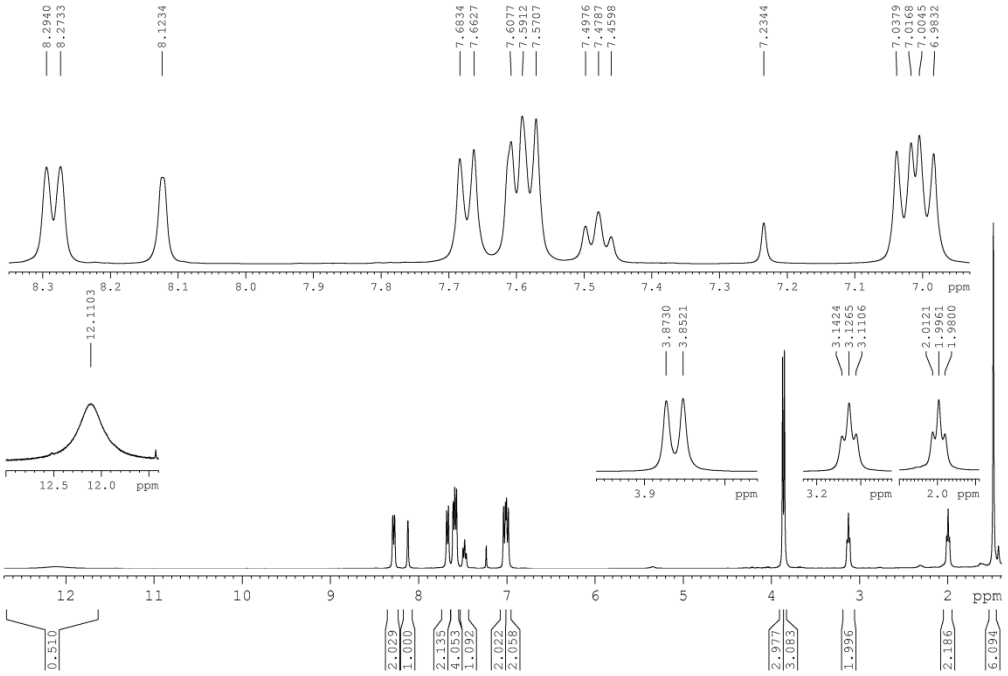

Figure S35. ^{1}H NMR spectrum of **P4** at 400 MHz in $CDCl_3$ (303 K).

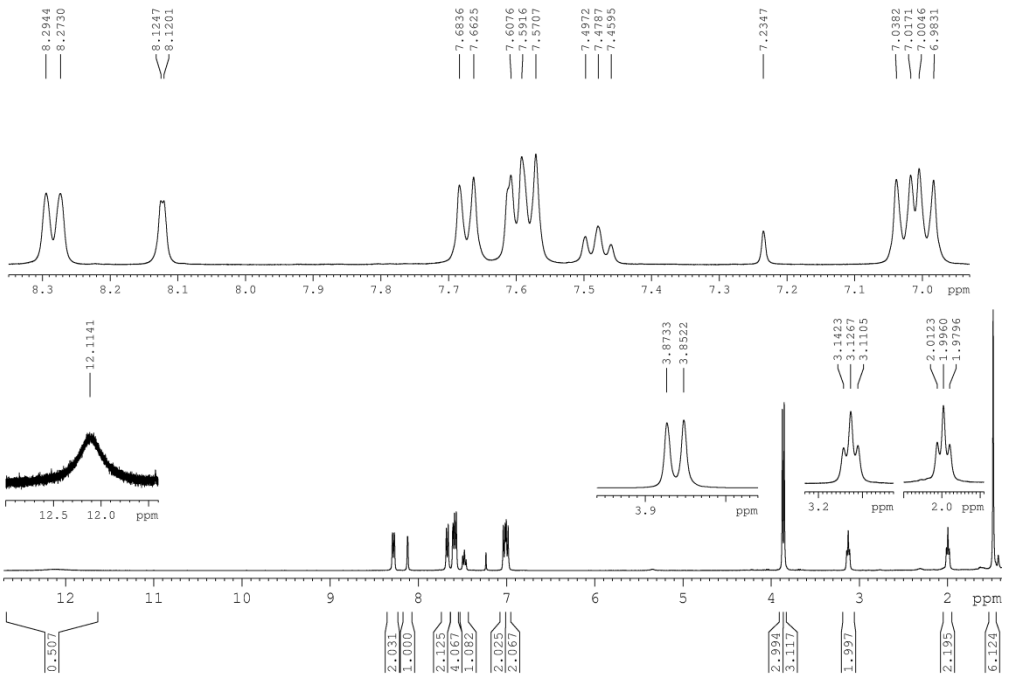

Figure S36. ^{1}H NMR spectrum of **P4** at 400 MHz in $CDCl_3$ (303 K).Lorentz-Gauss transformation (lb = -0.4, gb = 40 %).

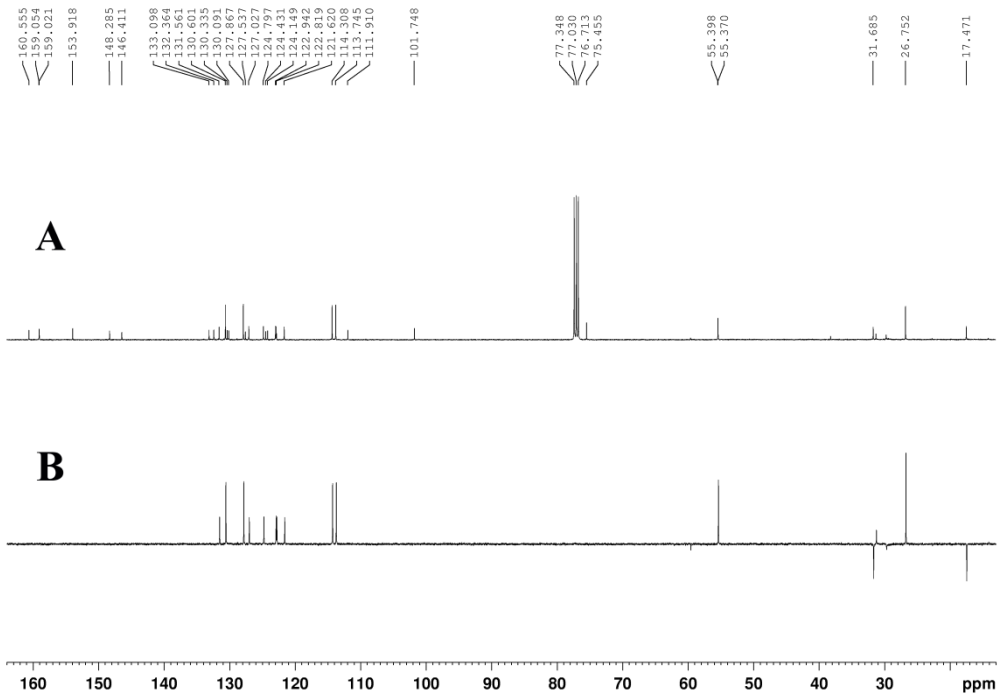

Figure S37. (A) ^{13}C NMR and (B) DEPT-135 spectra of **P4**at 100 MHz in $CDCl_3$ (303 K).

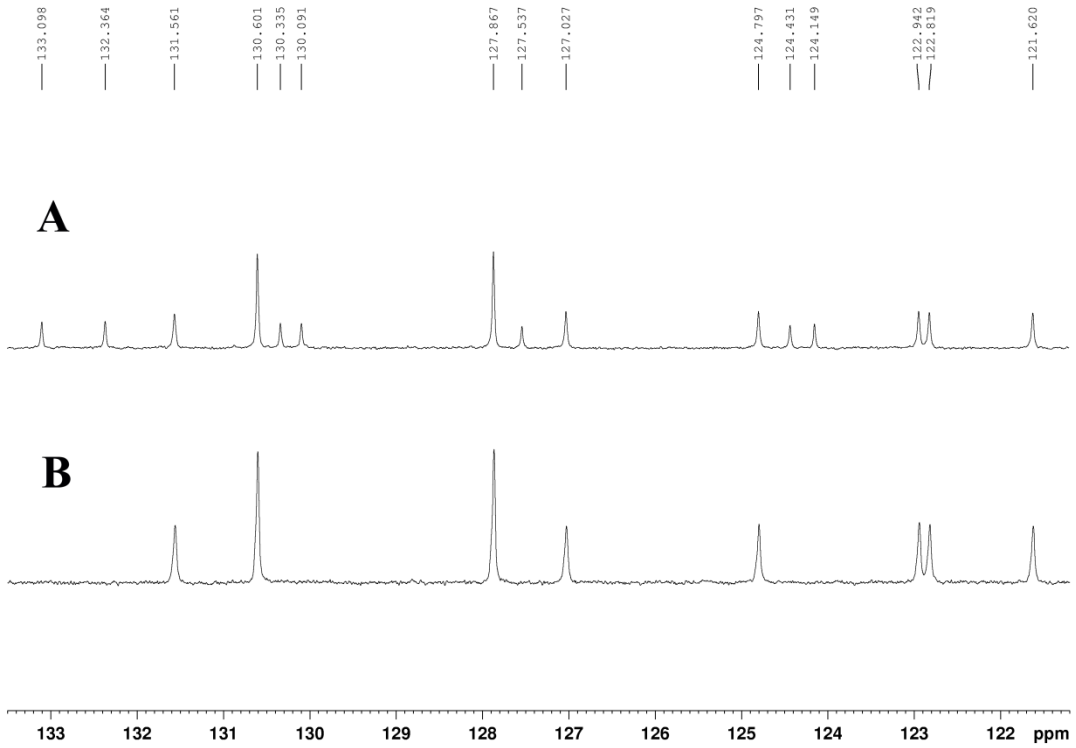

Figure S38. Expanded (A) ^{13}C NMR and (B) DEPT-135 spectra of **P4** at 100 MHz in $CDCl_3$ (303 K).

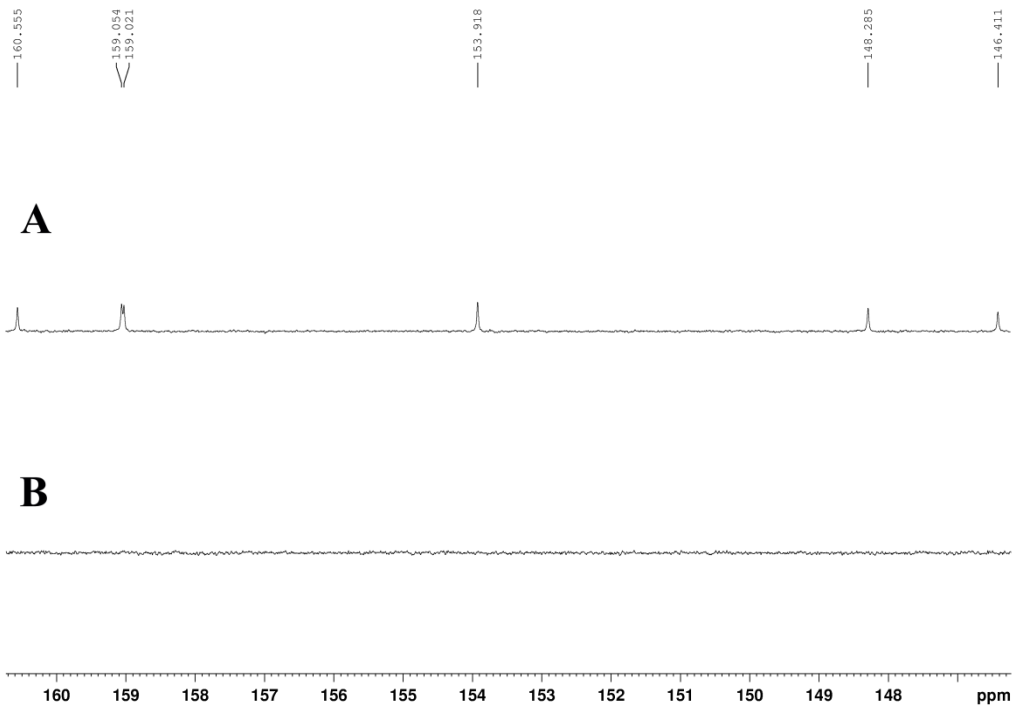

Figure S39. Expanded (A) ^{13}C NMR and (B) DEPT-135 spectra of **P4** at 100 MHz in $CDCl_3$ (303 K).

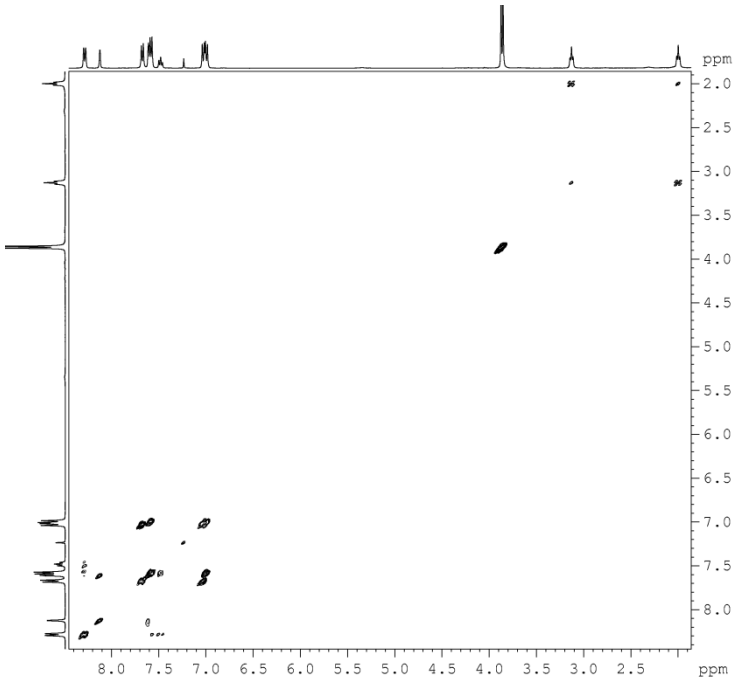

Figure S40. COSY spectrum of **P4** at 400 MHz in $CDCl_3$ (303 K).

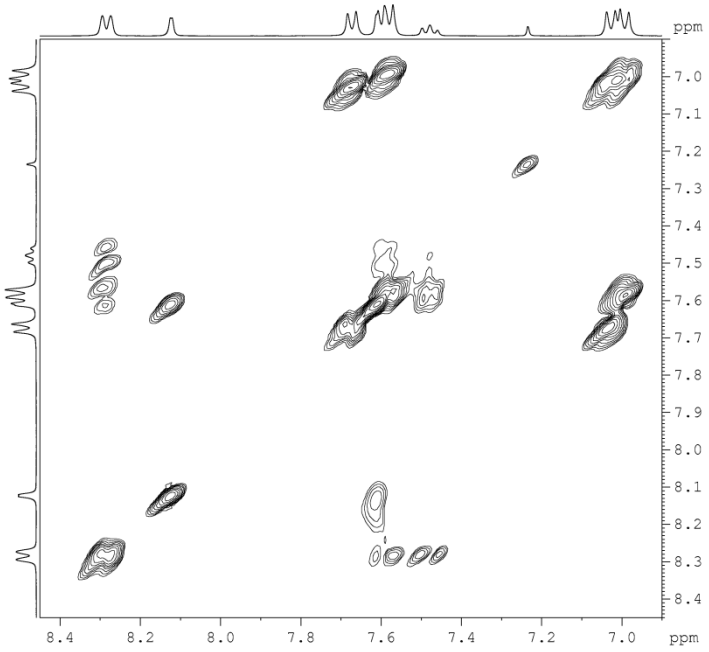

Figure S41. Expanded COSY spectrum of **P4** at 400 MHz in $CDCl_3$ (303 K) showing the correlations between aromatic ^1H resonances.

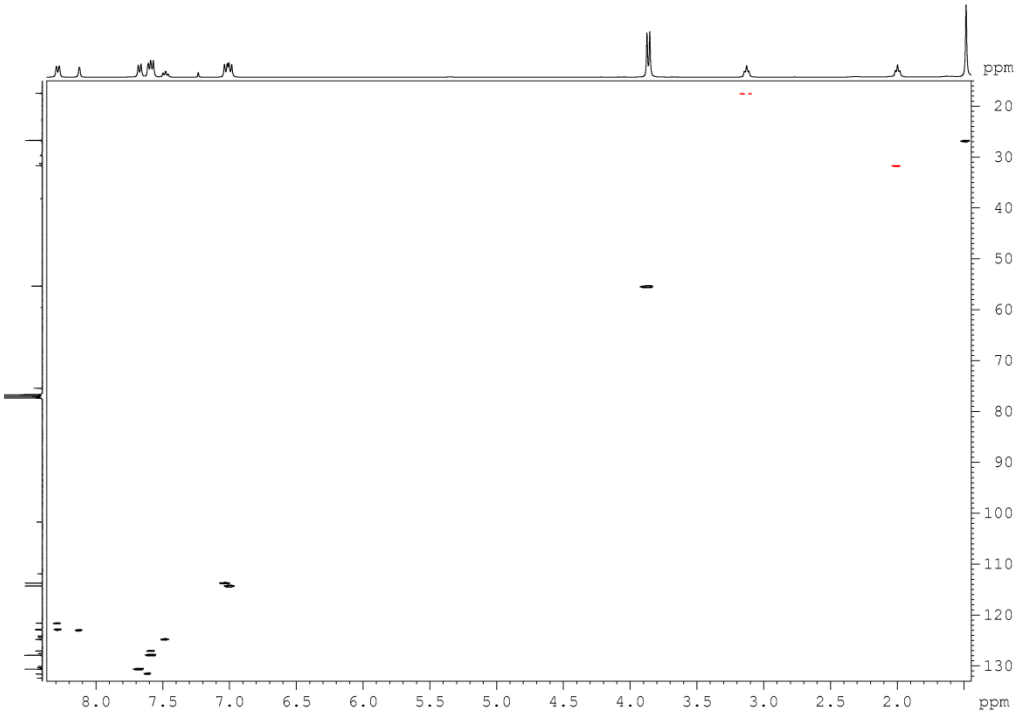

Figure S42. ^1H-^{13}C HSQC spectrum of **P4** at 400 MHz in $CDCl_3$ (303 K). Correlations in black represent peaks with positive phase (CH_3 and CH correlations) whereas the correlation in red indicates negative intensities (CH_2 correlations).

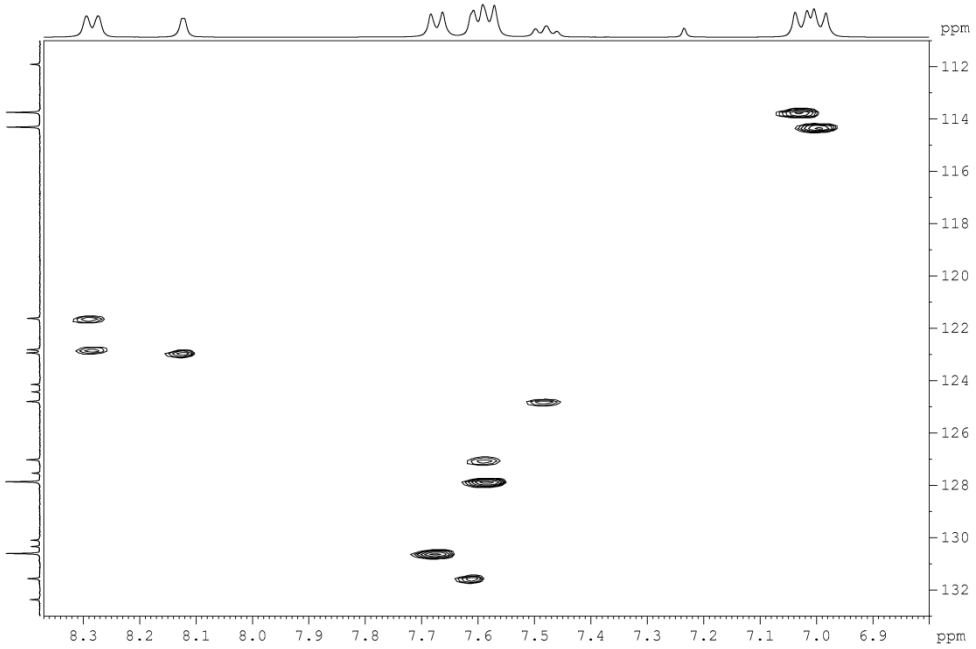

Figure S43. Expanded ^{1}H-^{13}C HSQC spectrum of **P4** at 400 MHz in $CDCl_3$ (303 K). Correlations in black represent peaks with positive phase (CH_3 and CH correlations) whereas the correlation in red indicates negative intensities (CH_2 correlations).

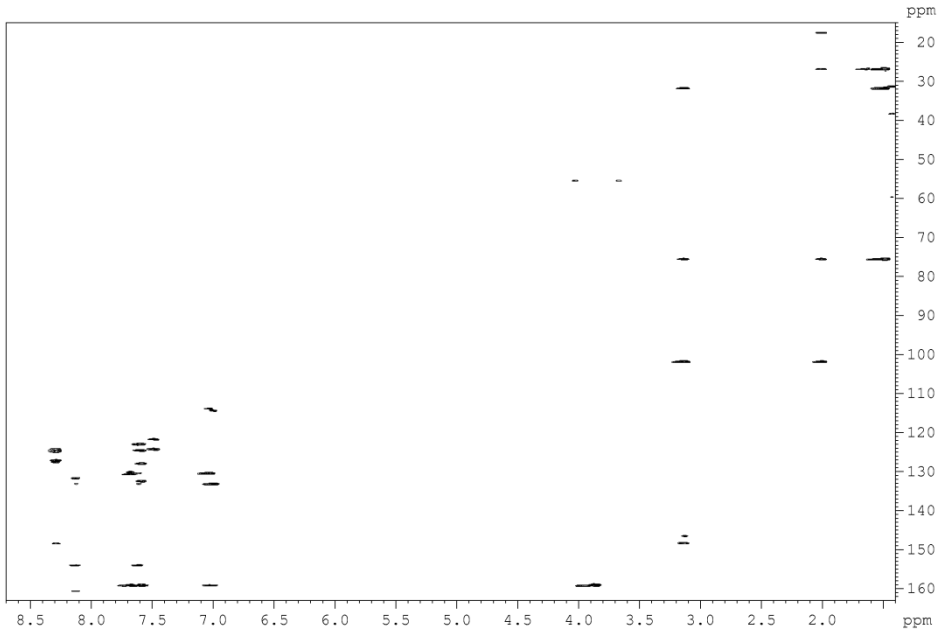

Figure S44. ^{1}H-^{13}C HMBC spectrum of **P4** at 400 MHz in $CDCl_3$ (303 K).

HRMS spectra

Compound P1

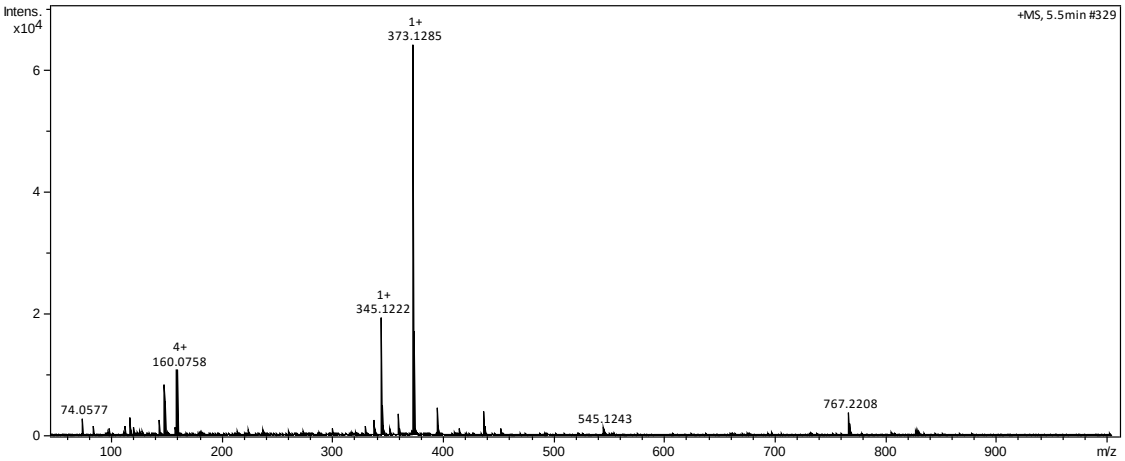

Figure S45. HRMS of **P1**.

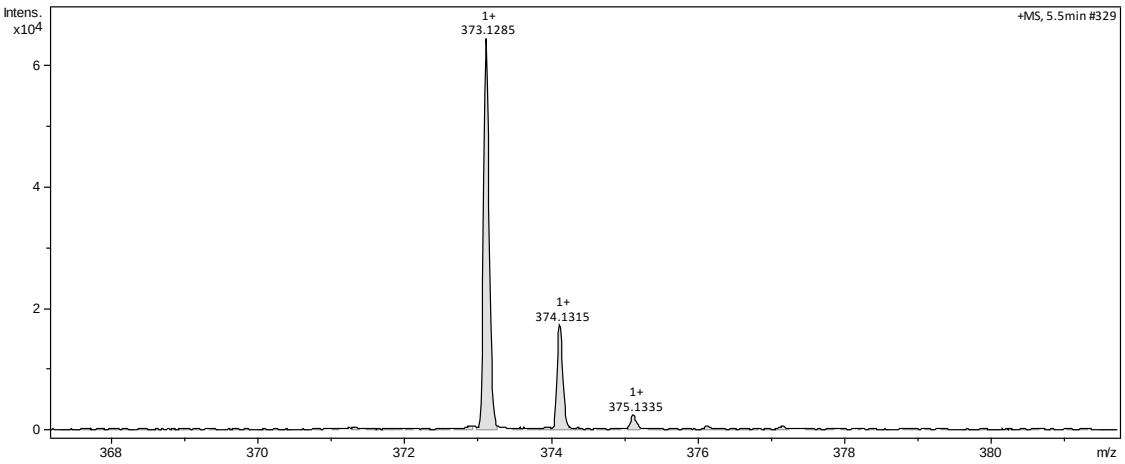

Figure S46. Expanded HRMS of **P1**.

Compound P2

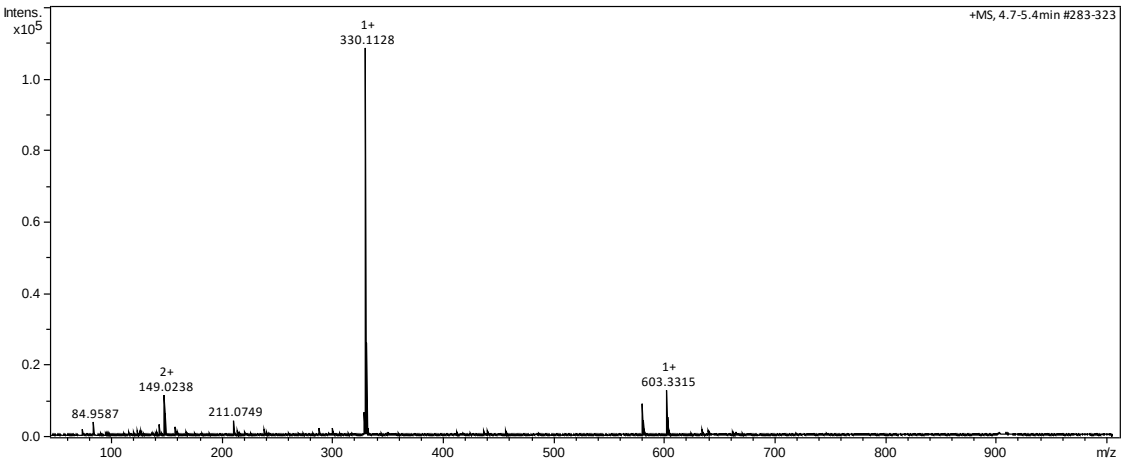

Figure S47. HRMS of **P2**.

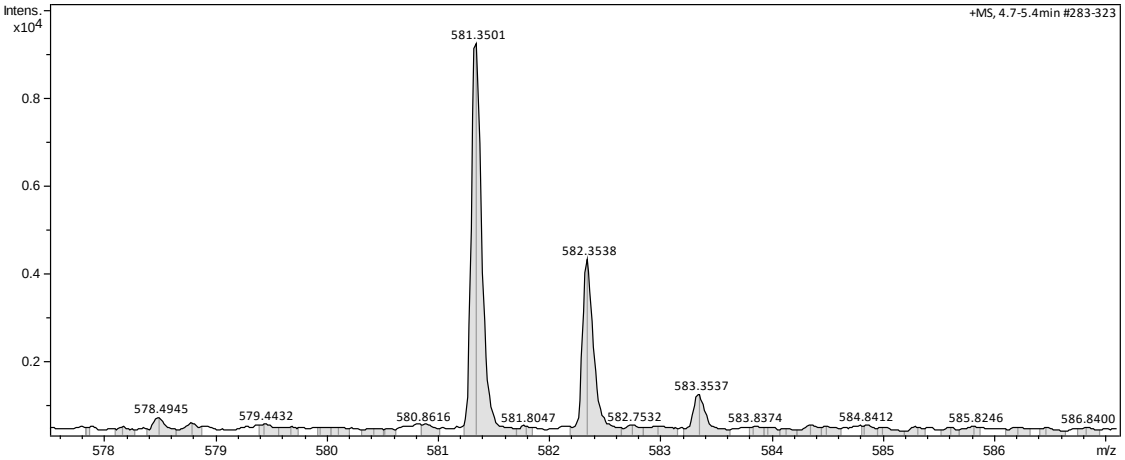

Figure S48. Expanded HRMS of **P2**.

Compound P3

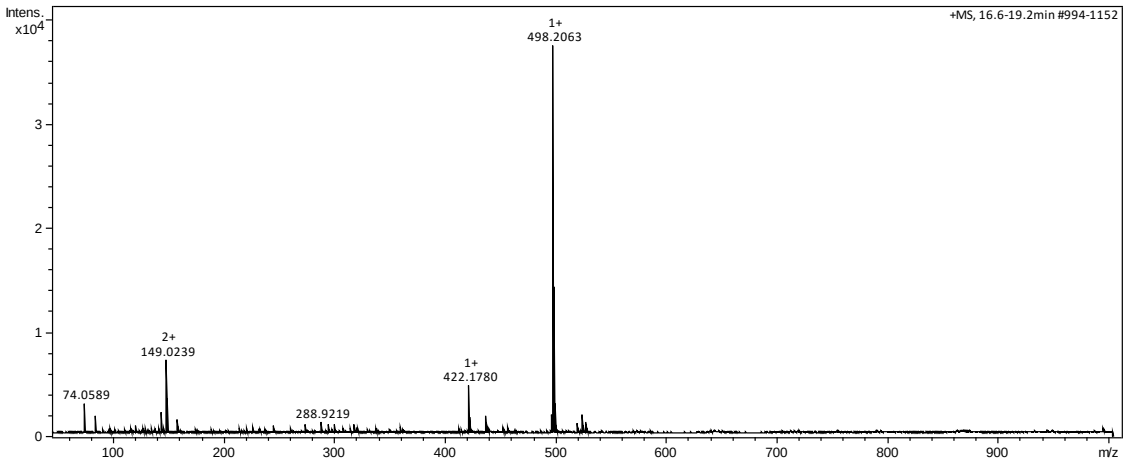

Figure S49. HRMS of **P3**.

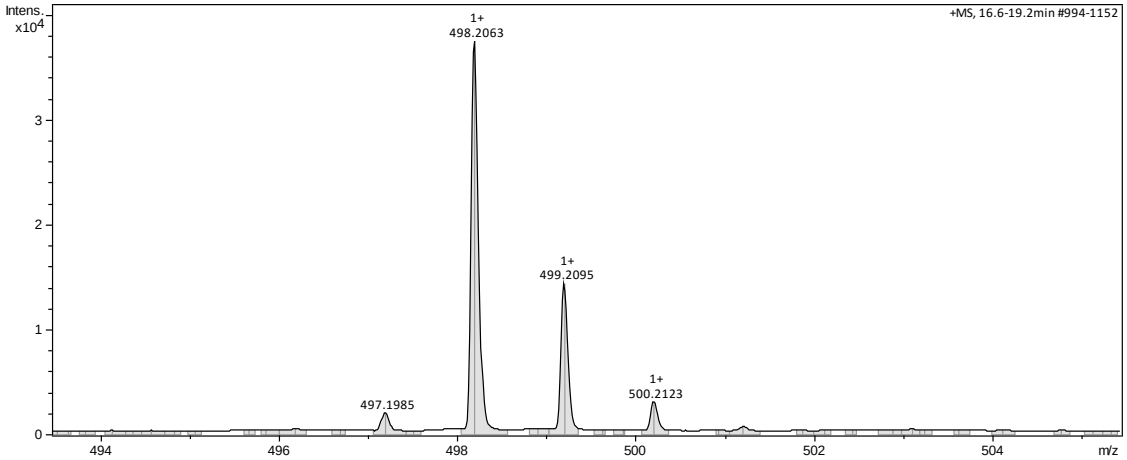

Figure S50. Expanded HRMS of **P3**.

Compound P4

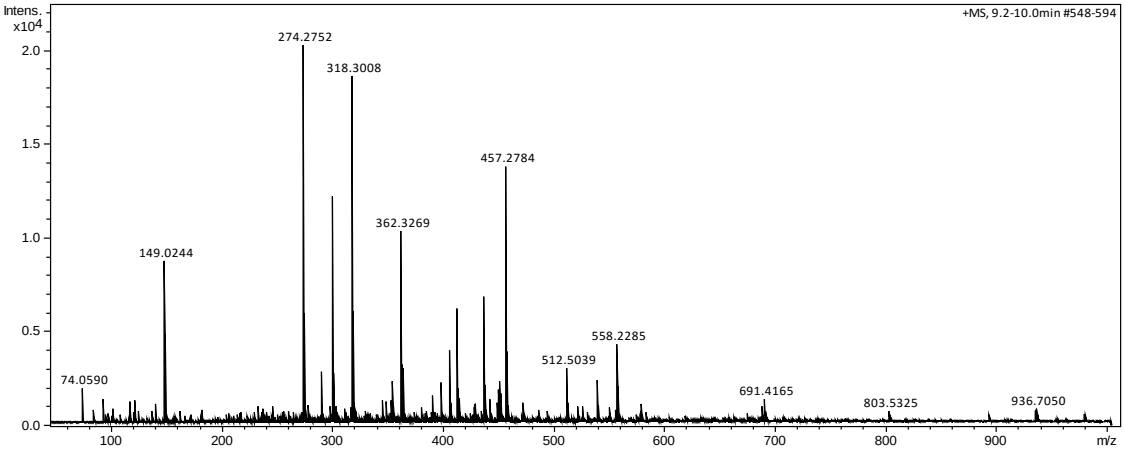

Figure S51. HRMS of **P4**.

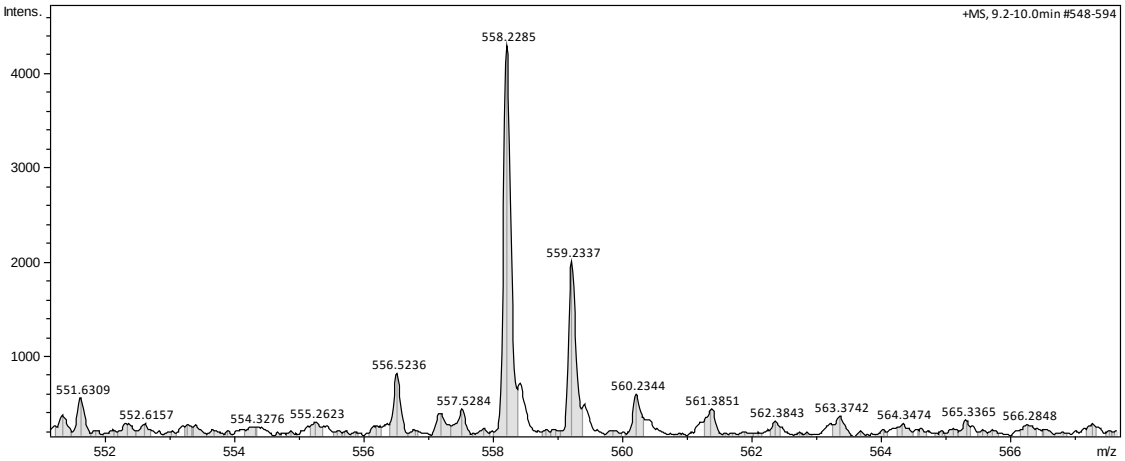

Figure S52. Expanded HRMS of **P4**.

Photophysical Analyses

Absorption spectra were obtained on a Varian Cary 100 spectrophotometer at room temperature in the solvents described below. Steady state fluorescence spectra were obtained on a Varian Cary Eclipse spectrofluorimeter with a xenon arc lamp as the light source while using an excitation wavelength (λ_{exc}) corresponding to a higher absorption band. In all experiments, a quartz cuvette was employed with a 1 cm optical path length. The absorbance and fluorescence emission for all of the compounds in seven different solvents with distinct polarities (ethyl acetate, acetonitrile, dichloromethane, hexane, toluene, methanol and dimethyl sulfoxide) were measured.

Studies on solvatochromism for each component tested, and for each solvent tested, a dichloromethane solution of the initial concentration of 5.00 x 10^{-6} mol L^{-1} was prepared. From **P1** and **P2** solution an aliquot of 1 mL was moved into a 10.0 mL volumetric flask. From **P3** and **P4** solution an aliquot of 0.10 mL was moved into a 10.0 mL. After the dichloromethane had completely evaporated, the volume of the balloon was completed with one of the tested solvents. For each sample in different solvents, the absorption and emission spectra were recorded.

Molar absorption and emission coefficients (ε) were obtained in dichloromethane. The absorbance of five solutions of known concentrations of **P1**, **P2**, **P3** and **P4** were obtained and plotted against the respective concentration, and ε was calculated from the slope of the regression analyses of the plotted data.

The respective calibration curves were built up for each molecule studied by absorption and emission spectroscopies. For **P1** and **P2** solutions with 1.0; 2.0; 3.0; 4.0 and 5.0x10^{-5} mol L^{-1} concentrations were prepared. For **P3** and **P4**, the following concentrations were prepared: 1.0; 2.0; 3.0; 4.0 and 5.0x10^{-6} mol L^{-1}.

Quantum yields of **P1** and **P2** were obtained by a comparative method[1] using 500 x 10^{-6} mol L^{-1} quinine sulfate in 0.1 mol L^{-1} and H_2SO_4 (aq) as standard[2] (φ = 0.54[3]). Fluorescein 500 x 10^{-6} mol L^{-1} in 0.1 mol L^{-1} of NaOH (aq) was used as standard (φ = 0.79) for recorded quantum yields of **P3** e **P4**.[4]

The emission spectra from four samples of each fluorophore (absorbance between 0.17 and 0.015 at the excitation wavelength) were obtained. The results were plotted with the integrated fluorescence intensity vs. absorbance to obtain the slope of the curve. A curve was obtained for each tested compound as well as for the standard. The quantum yield of the tested compound (Φ_x) was calculated using the following formula, where Φ_{St}

is the quantum yield of the standard, m_x and m_{St} are the slopes for the test compound and standard compound, respectively, and n_x and n_{st} are the refractive indexes of the solvents.

$$\Phi_X = \Phi_{St}\left[\frac{m_x}{m_{St}}\right]\left[\frac{n_x}{n_{St}}\right]^2 \qquad (1)$$

Photophysical properties of the **P1**, **P2**, **P3** and **P4** were studied in seven different solvents, which varied in polarity and were either protic or aprotic: ethyl acetate, hexane, dichloromethane, acetonitrile, dimethyl sulfoxide, methanol and toluene. The four studied compounds, regardless of the solvent, showed strong absorptions in the ultraviolet (300-400 nm) as well as strong fluorescent emissions, which are visible to the naked eye, in the blue region (400-500 nm) for **P1** and **P2**; and green-yellow region (500-600 nm) for **P3** and **P4**.

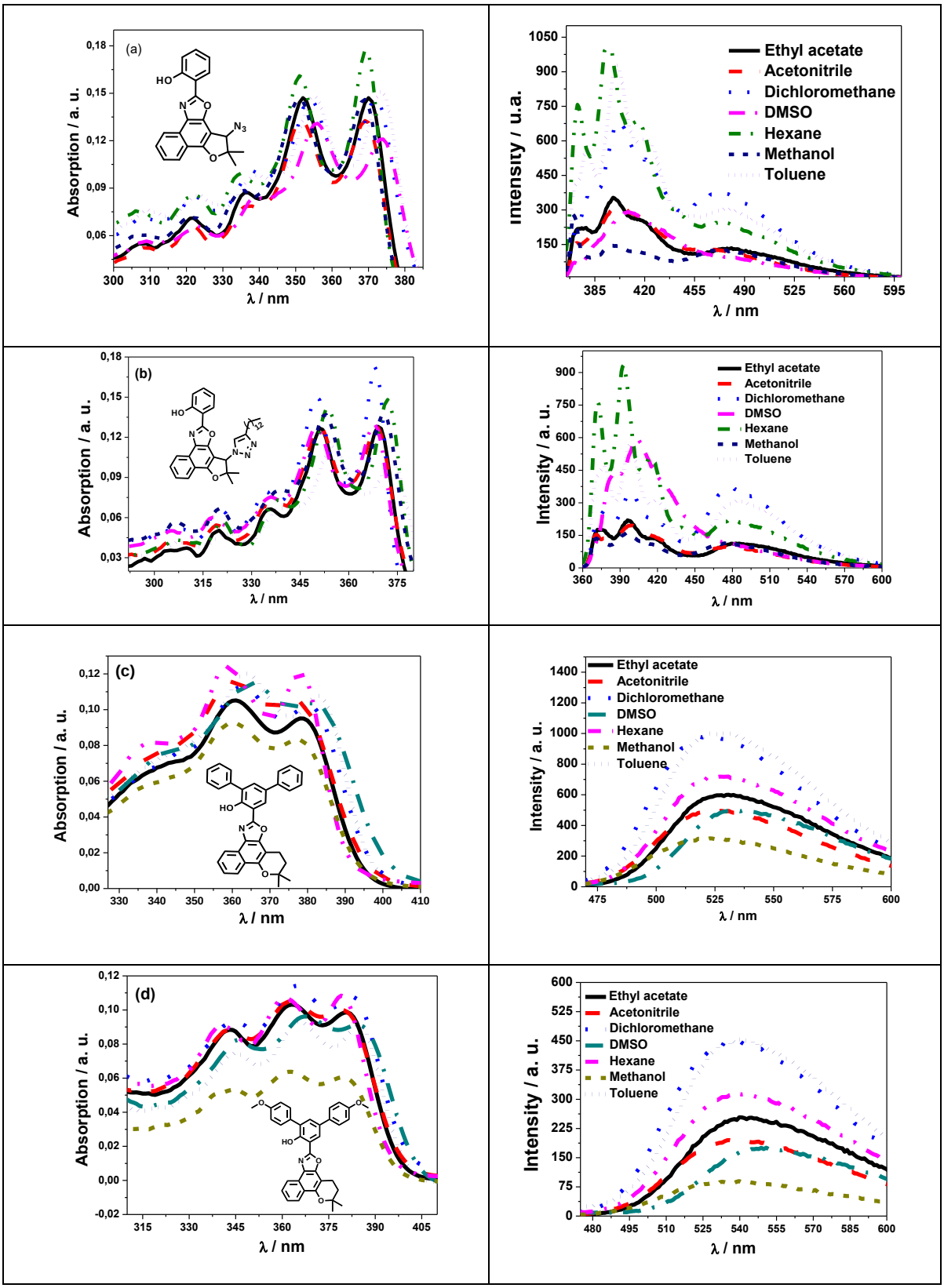

Figure S53. UV-Vis spectra (left) and emission spectra (right) of (a) **P1**, (b) **P2**, (c) **P3** and (d) **P4** in different solvents.

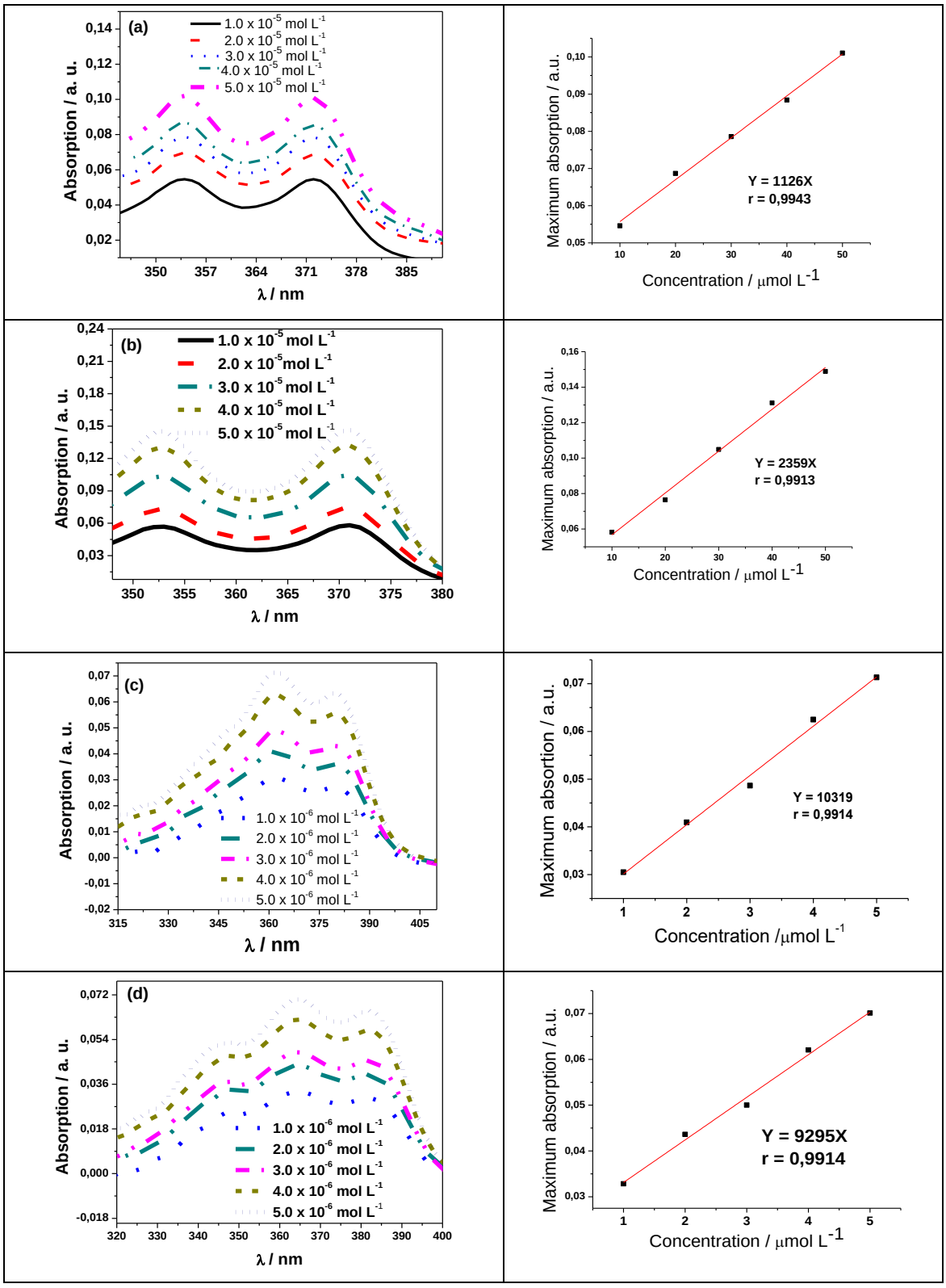

Figure S54. UV-Vis spectra (left) and calibration curve (right) for (a) **P1**, (b) **P2**, (c) **P3** and (d) **P4**.

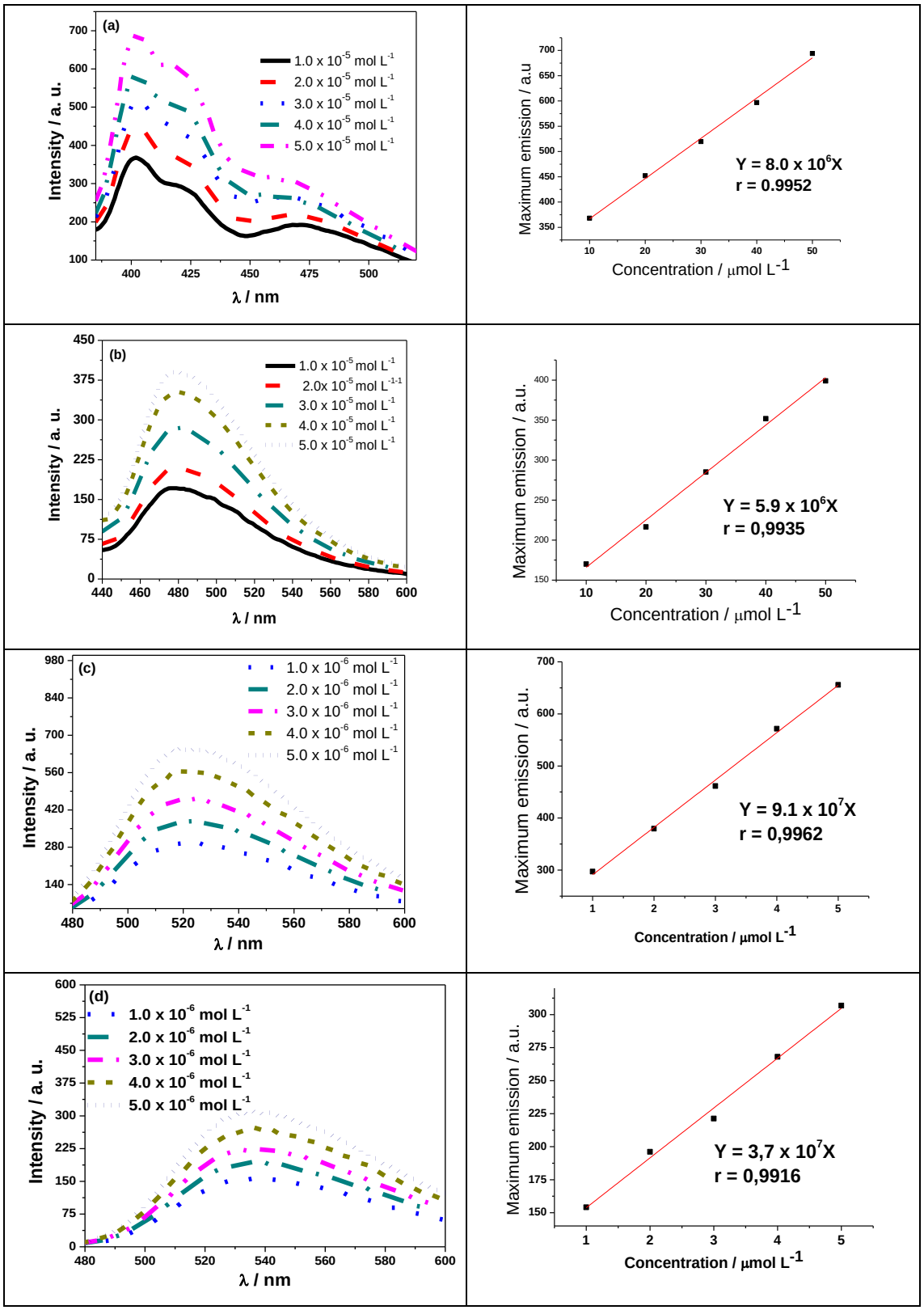

Figure S55. Emission spectra (left) and calibration curve (right) obtained for (a) **P1**, (b) **P2**, (c) **P3** and (d) **P4**.

Computational details

The oxazoles derivatives were fully optimized using the density functional theory as implemented in Gaussian 09 series of programs.[5] The generalized gradient approximation for the exchange/correlation (XC) functional due to Perdew, Burke and Ernzerhof (PBEPBE)[6,7] where used in combination with the Dunning's double zeta cc_pVDZ basis sets.[8] Frequency analyses were performed in the harmonic approach for all studied molecules. Real frequencies assure that a minimum in the potential energy surface was found. The optimized geometries of the ground (S_0) and first excited (S_1) states were employed for the single point TD-DFT calculations. The polarizable continuum model (PCM)[9] where included to include the implicit solvent effects. The dielectric constant of DMSO (ε = 46.826) was used.

Table S5. Calculated properties of the different compounds in the ground and first excited states. The geometries were fully optimized at the PBEPBE/cc-pVDZ level of theory.

Compounds	XC	State	μ(D)	HOMO(eV)	LUMO(eV)	Absortion/ Emission (nm)
P1	PBEPBE	S_0	2.10	-4.7840	-2.3243	433.09
		S_1	2.94	-4.6253	-2.4678	491.83
P2	PBEPBE	S_0	1.70	-4.8798	-2.3946	425.52
		S_1	2.89	-4.7233	-2.5565	488.89
P3	PBEPBE	S_0	2.52	-4.6478	-2.2144	456.47
		S_1	7.06	-4.5280	-2.3772	525.43
P4	PBEPBE	S_0	2.74	-4.4242	-2.0861	477.66
		S_1	4.92	-4.264	-2.2705	554.40

Cartesian coordinates for the calculated structures at the ground state.

Compound P1 – PBEPBE/cc-pVDZ at DMSO.

SCF Done: E(RPBE-PBE) = -1253.16040298 a.u. after 1 cycles
Convg = 0.4222D-07 1 Fock formations.
S**2 = 0.0000 -V/T = 2.0063

Standard orientation:

Center Number	Atomic Number	Atomic Type	Coordinates (Angstroms) X	Y	Z
1	6	0	-3.842394	-1.543102	0.244071
2	6	0	-3.423356	-0.193433	0.152958
3	6	0	-4.401292	0.851094	0.081653
4	6	0	-5.769357	0.505513	0.114070
5	6	0	-6.160814	-0.834246	0.207609
6	6	0	-5.200393	-1.865980	0.270901
7	6	0	-2.027491	0.176978	0.123908
8	8	0	-1.052077	-0.799610	0.227426
9	6	0	0.131469	-0.103300	0.154488
10	6	0	-0.159949	1.259515	0.009787
11	7	0	-1.544652	1.405065	-0.000851
12	6	0	1.440940	-0.605522	0.200272
13	6	0	2.465145	0.330852	0.070605
14	6	0	2.248669	1.742284	-0.079333
15	6	0	0.886283	2.229304	-0.112855
16	6	0	2.038032	-1.983996	0.269481
17	6	0	3.560346	-1.657098	0.469279
18	8	0	3.707207	-0.215949	0.096608
19	6	0	0.659906	3.623450	-0.265841
20	6	0	1.730645	4.504175	-0.380204
21	6	0	3.066929	4.026598	-0.344535
22	6	0	3.321709	2.667881	-0.195924
23	6	0	3.922525	-1.753445	1.951882
24	6	0	4.510563	-2.439274	-0.423480
25	7	0	1.809618	-2.759131	-0.995106
26	7	0	0.728050	-3.355324	-1.066312
27	7	0	-0.242087	-3.956665	-1.256929
28	8	0	-4.061207	2.153416	-0.015927
29	1	0	4.352357	2.288050	-0.166448
30	1	0	3.902691	4.735167	-0.433549
31	1	0	1.540703	5.580800	-0.498323
32	1	0	-0.375122	3.992458	-0.292007
33	1	0	-6.510031	1.315892	0.061090
34	1	0	-7.232509	-1.080873	0.229260
35	1	0	-5.516360	-2.915895	0.339345
36	1	0	-3.077217	-2.331066	0.283829
37	1	0	-3.048093	2.193470	-0.037696
38	1	0	3.876127	-2.808477	2.286948
39	1	0	4.949461	-1.375548	2.117891
40	1	0	3.221462	-1.159519	2.571358
41	1	0	5.549290	-2.097743	-0.251093
42	1	0	4.453320	-3.519298	-0.187349

43	1	0	4.254568	-2.303666	-1.490066
44	1	0	1.662773	-2.583704	1.123581

Compound P2 – PBEPBE/cc-pVDZ at DMSO.

SCF Done: E(RPBE-PBE) = -1840.86456480 a.u. after 1 cycles
Convg = 0.8068D-07 1 Fock formations.
S**2 = 0.0000 -V/T = 2.0069

Standard orientation:

Center Number	Atomic Number	Atomic Type	Coordinates (Angstroms) X	Y	Z
	1	6	0	-6.750925	-0.734159	2.816436
	2	6	0	-5.883964	-0.266673	1.791127
	3	6	0	-5.370836	1.083959	1.856973
	4	6	0	-5.746207	1.907436	2.952160
	5	6	0	-6.593585	1.420982	3.942284
	6	6	0	-7.099525	0.096350	3.875431
	7	6	0	-4.508515	1.510268	0.796683
	8	6	0	-4.171741	0.649686	-0.256727
	9	6	0	-4.650839	-0.667847	-0.345605
10	6	0	-5.492441	-1.090782	0.683191
11	7	0	-3.868894	2.726870	0.579663
12	6	0	-3.191069	2.571499	-0.548671
13	8	0	-3.332050	1.316532	-1.116755
14	8	0	-5.913073	-2.375705	0.551433
15	6	0	-5.514148	-2.843041	-0.808297
16	6	0	-4.418221	-1.811846	-1.290288
17	6	0	-2.363461	3.568369	-1.187572
18	6	0	-1.670921	3.313609	-2.396375
19	6	0	-0.880857	4.301641	-2.986627
20	6	0	-0.773900	5.565865	-2.369362
21	6	0	-1.448552	5.839777	-1.175059
22	6	0	-2.252132	4.853706	-0.563244
23	8	0	-2.887334	5.156271	0.587942
24	7	0	-3.033414	-2.302482	-1.243315
25	6	0	-6.754520	-2.720441	-1.693354
26	6	0	-5.031314	-4.277427	-0.665611
27	1	0	-7.137809	-1.760614	2.754079
28	1	0	-7.770695	-0.272323	4.664096
29	1	0	-6.875809	2.068948	4.784682
30	1	0	-5.355756	2.933607	3.002274
31	1	0	-1.371383	6.821286	-0.686377
32	1	0	-0.153401	6.349511	-2.828323
33	1	0	-0.347462	4.093864	-3.924245
34	1	0	-1.767027	2.322323	-2.860745
35	1	0	-3.406363	4.329658	0.864769
36	1	0	-6.532178	-3.095643	-2.711941
37	1	0	-7.583767	-3.318823	-1.270407
38	1	0	-7.082934	-1.665166	-1.773840
39	1	0	-5.862112	-4.919435	-0.315678
40	1	0	-4.680847	-4.658571	-1.644094

41	1	0	-4.197675	-4.351533	0.058101
42	1	0	-4.584715	-1.564001	-2.355802
43	7	0	-2.487510	-2.852554	-2.359931
44	7	0	-1.272602	-3.252816	-2.047433
45	6	0	-1.023399	-2.969135	-0.723923
46	6	0	-2.156427	-2.357481	-0.197185
47	1	0	-2.396069	-1.966854	0.794777
48	6	0	0.298168	-3.259077	-0.078058
49	1	0	0.182722	-3.216192	1.024614
50	1	0	0.599704	-4.298970	-0.328176
51	6	0	1.411092	-2.291200	-0.524755
52	6	0	2.769820	-2.591873	0.115868
53	1	0	1.498789	-2.335459	-1.632764
54	1	0	1.104884	-1.249321	-0.282006
55	6	0	3.879974	-1.633618	-0.331207
56	1	0	2.670892	-2.550594	1.224683
57	1	0	3.066270	-3.638782	-0.122817
58	6	0	5.240468	-1.915442	0.317041
59	1	0	3.982834	-1.682962	-1.439333
60	1	0	3.574927	-0.586769	-0.102852
61	6	0	6.348583	-0.956524	-0.133915
62	1	0	5.137098	-1.862849	1.425111
63	1	0	5.545733	-2.962971	0.091884
64	6	0	7.708209	-1.227113	0.520916
65	1	0	6.456018	-1.014226	-1.241364
66	1	0	6.038471	0.091136	0.084308
67	6	0	8.814492	-0.267008	0.067957
68	1	0	7.600769	-1.167662	1.628310
69	1	0	8.018895	-2.274880	0.304124
70	6	0	10.173602	-0.531404	0.726384
71	1	0	8.924230	-0.329121	-1.039067
72	1	0	8.501172	0.780767	0.281081
73	6	0	11.278454	0.430043	0.272881
74	1	0	10.063682	-0.468878	1.833380
75	1	0	10.487498	-1.579036	0.513507
76	6	0	12.637418	0.169049	0.932420
77	1	0	11.389071	0.366448	-0.834019
78	1	0	10.963028	1.477585	0.484221
79	6	0	13.741608	1.131955	0.479565
80	1	0	12.527412	0.232238	2.039597
81	1	0	12.954452	-0.878115	0.720647
82	6	0	15.093968	0.862037	1.144810
83	1	0	13.850195	1.068034	-0.626593
84	1	0	13.423203	2.177471	0.691581
85	1	0	15.871274	1.573049	0.798490
86	1	0	15.024476	0.953285	2.249488
87	1	0	15.454742	-0.164208	0.921053

Compound P3 – PBEPBE/cc-pVDZ at DMSO.

SCF Done: E(RPBE-PBE) = -1590.53030826 a.u. after 1 cycles
Convg = 0.1134D-06 1 Fock formations.
S**2 = 0.0000 -V/T = 2.0067

Standard orientation:

Center Number	Atomic Number	Atomic Type	Coordinates (Angstroms) X	Y	Z
1	6	0	-5.577980	-2.306599	-0.020968
2	6	0	-4.423138	-1.474500	-0.028459
3	6	0	-3.124768	-2.104444	-0.005082
4	6	0	-3.030987	-3.521560	0.019588
5	6	0	-4.180446	-4.304357	0.022358
6	6	0	-5.460010	-3.692576	0.003110
7	6	0	-1.996905	-1.228891	-0.005123
8	6	0	-2.185631	0.154409	-0.032711
9	6	0	-3.426574	0.821992	-0.067553
10	6	0	-4.542955	-0.027320	-0.060732
11	7	0	-0.629416	-1.484899	0.005643
12	6	0	-0.050739	-0.292072	-0.016280
13	8	0	-0.943803	0.759485	-0.039165
14	8	0	-5.823494	0.438879	-0.105115
15	6	0	-6.052611	1.881024	0.138291
16	6	0	-4.977466	2.692887	-0.602524
17	6	0	1.374355	-0.039721	-0.026082
18	6	0	1.890326	1.273267	-0.038464
19	6	0	3.274925	1.510191	-0.034703
20	6	0	4.131399	0.382607	-0.020677
21	6	0	3.665224	-0.945348	-0.010960
22	6	0	2.256874	-1.168075	-0.009156
23	8	0	1.784634	-2.429548	0.022285
24	6	0	-6.034209	2.105961	1.654765
25	6	0	-7.440451	2.135665	-0.444373
26	1	0	-6.567388	-1.831273	-0.033940
27	1	0	-6.364620	-4.317726	0.009052
28	1	0	-4.097558	-5.400733	0.041454
29	1	0	-2.034471	-3.985484	0.036843
30	6	0	4.639100	-2.072761	0.005126
31	1	0	5.218481	0.541999	-0.064724
32	6	0	3.823103	2.892126	-0.055870
33	1	0	1.181209	2.112019	-0.030794
34	1	0	0.765722	-2.367692	0.023592
35	1	0	-6.217239	3.174719	1.884286
36	1	0	-6.826741	1.503597	2.139981
37	1	0	-5.062453	1.819214	2.101756
38	1	0	-8.191049	1.479779	0.038856
39	1	0	-7.736746	3.188706	-0.272508
40	1	0	-7.450270	1.941531	-1.534713
41	6	0	-3.564605	2.320359	-0.142974
42	1	0	-5.084287	2.493294	-1.689057
43	1	0	-5.168237	3.772847	-0.447313
44	1	0	-2.808440	2.733410	-0.841276

45	1	0	-3.338948	2.773458	0.847144
46	6	0	5.033748	3.207026	0.606544
47	6	0	5.552058	4.510153	0.584979
48	6	0	4.871525	5.533519	-0.095646
49	6	0	3.667007	5.238067	-0.755956
50	6	0	3.150868	3.934132	-0.738383
51	1	0	5.565883	2.424861	1.167928
52	1	0	6.491585	4.729208	1.113636
53	1	0	5.277449	6.555443	-0.111502
54	1	0	3.128053	6.027848	-1.299998
55	1	0	2.221754	3.714604	-1.284852
56	6	0	5.800032	-1.992329	0.810410
57	6	0	6.754156	-3.020751	0.810241
58	6	0	6.569651	-4.155688	0.003826
59	6	0	5.420730	-4.250842	-0.799434
60	6	0	4.464301	-3.225173	-0.797607
61	1	0	5.946110	-1.117345	1.461190
62	1	0	7.644306	-2.936467	1.451074
63	1	0	7.315814	-4.963708	0.003609
64	1	0	5.267321	-5.133057	-1.438626
65	1	0	3.572545	-3.311548	-1.431768

Compound P4 – PBEPBE/cc-pVDZ at DMSO.

SCF Done: E(RPBE-PBE) = -1819.33657271 a.u. after 1 cycles
Convg = 0.9865D-07 1 Fock formations.
S**2 = 0.0000 -V/T = 2.0066

Standard orientation:

Center Number	Atomic Number	Atomic Type	Coordinates (Angstroms) X	Y	Z
	1	6	0	3.898207	-3.190982	0.713072
	2	6	0	4.038622	-2.004899	-0.041569
	3	6	0	5.230212	-1.854984	-0.796233
	4	6	0	6.228044	-2.830850	-0.791488
	5	6	0	6.071852	-4.006387	-0.024318
	6	6	0	4.894127	-4.179795	0.731362
	7	6	0	3.018409	-0.921711	-0.034644
	8	6	0	3.426672	0.426453	-0.038857
	9	6	0	2.526800	1.520446	-0.051671
10	6	0	1.152894	1.227652	-0.052230
11	6	0	0.692075	-0.106743	-0.041445
12	6	0	1.618748	-1.198553	-0.037139
13	6	0	-0.721968	-0.414926	-0.058723
14	7	0	-1.256278	-1.628604	-0.061047
15	6	0	-2.632467	-1.423187	-0.077929
16	6	0	-2.872732	-0.047775	-0.084599
17	8	0	-1.654422	0.603027	-0.072733
18	6	0	-4.137832	0.573631	-0.112818
19	6	0	-5.221676	-0.316654	-0.121068
20	6	0	-5.047839	-1.758466	-0.111621
21	6	0	-3.726876	-2.339996	-0.095175

22	6	0	-3.580492	-3.752950	-0.091395
23	6	0	-4.699988	-4.577912	-0.102257
24	6	0	-6.001477	-4.013814	-0.114929
25	6	0	-6.170955	-2.633020	-0.118753
26	8	0	-6.519127	0.101675	-0.159315
27	6	0	-6.801933	1.529396	0.110078
28	6	0	-5.758362	2.394083	-0.615987
29	6	0	-4.332255	2.067010	-0.162834
30	6	0	-6.791305	1.727970	1.630324
31	6	0	-8.198510	1.742884	-0.468289
32	6	0	3.021656	2.921131	-0.053432
33	6	0	4.228141	3.275361	-0.708915
34	6	0	4.697241	4.590090	-0.714367
35	6	0	3.971936	5.611274	-0.061089
36	6	0	2.768520	5.283678	0.596728
37	6	0	2.312428	3.956096	0.594315
38	8	0	1.194950	-2.479573	-0.050024
39	1	0	-7.177388	-2.194726	-0.126528
40	1	0	-6.882277	-4.672135	-0.119747
41	1	0	-4.576519	-5.670637	-0.098983
42	1	0	-2.567240	-4.179226	-0.079029
43	1	0	4.505645	0.632358	0.012246
44	1	0	0.410305	2.036509	-0.080156
45	1	0	0.175628	-2.457025	-0.057503
46	1	0	-7.015635	2.784550	1.878869
47	1	0	-7.559573	1.086783	2.104732
48	1	0	-5.808824	1.471250	2.072087
49	1	0	-8.924235	1.051079	0.002695
50	1	0	-8.533240	2.781037	-0.277511
51	1	0	-8.201256	1.568269	-1.561988
52	1	0	-5.858095	2.209147	-1.705795
53	1	0	-5.989579	3.463343	-0.442476
54	1	0	-3.592627	2.520176	-0.853960
55	1	0	-4.122904	2.511058	0.834981
56	1	0	4.801767	2.507584	-1.248816
57	1	0	5.628599	4.857198	-1.234092
58	8	0	4.516629	6.863698	-0.125407
59	1	0	2.185234	6.049238	1.124272
60	1	0	1.385216	3.721726	1.138003
61	1	0	5.368971	-0.958968	-1.419190
62	1	0	7.142941	-2.709435	-1.389017
63	8	0	7.103681	-4.900563	-0.088523
64	1	0	4.742076	-5.079528	1.341430
65	1	0	2.991356	-3.346815	1.311013
66	6	0	3.806481	7.927216	0.517294
67	1	0	4.405666	8.837962	0.339972
68	1	0	2.792552	8.063339	0.082961
69	1	0	3.714409	7.754947	1.611389
70	6	0	6.979737	-6.109488	0.667865
71	1	0	7.904359	-6.681333	0.473022
72	1	0	6.896732	-5.904063	1.756947
73	1	0	6.101354	-6.707218	0.341931

Cellular experimental procedures

Cell lineage maintenance

It was used Caco-2 (adenocarcinoma colorectal cells). Caco-2 cells were purchase from "Associção Técnico Científica Paul Ehrlich APABCAM". Cells were maintained according to ATCC (American Type Culture Collection) recommendations at 37º C in atmosphere with 5% CO_2.

Solubility test

Four solvents was used in this test i.e. water, acetone, dimethyl sulfoxide and hexane. It was used the mass of 1 mg from each compound to 1 mL of diluent. This assay was performed at room temperature or under 60 ºC heat and under severe stirring for the both conditions. If the compound was soluble in one of those solvents the test was stopped and this solvent adopted as standard solvent to this compound. It was considered soluble the solution in which it was not possible found any precipitate at naked eyes.

Fluorescence assay

The cell samples were seeded on 13 mm round glass coverslips on the bottom of a 24-well plate, allowed to adhere overnight and washed three times with serum-free medium for removal of non-adherent cells. After reaching confluence, the cells were whased three times in PBS 1X (pH 7.4) and then fixed in formaldehyde 3.7 % for 30 minutes. After fixative procedure the samples were washed three times in PBS 1X (pH 7.4) at room temperature and incubated for 30 minutes with the compounds **P1**, **P2**, **P3** and **P4** solution at 100 μM. The samples were washed three times in PBS 1X (pH 7.4) at room temperature and the coverslips were mounted over glass slides using ProLong Gold Antifade (Invitrogen, OR, USA) according to the manufacturer's recommendations. The negative control was performed by incubation of the samples in hexane, which was the diluent used. The samples were analyzed using a Leica Confocal Microscopy TCS SP5 and excited using 488 nM wavelength laser emission. All assays were performed in triplicate and it was done three repetitions for each experimental condition.

Lipid inclusion staining with Bodipy

The lipid inclusion staining procedures were performed with commercially available BODIPY. Briefly, the cells samples were incubated with BODIPY and DMSO solution (12.6 μM – down to 0.1% in the final dilution) during 30 minutes at room temperature. After samples incubation, the cells were washed three times in PBS and the samples were mounted over glass slides by using antifade agent Prolong Gold (Invitrogen, OR, USA) according to the manufacture's recommendations. The samples were analyzed using a Leica Confocal Microscopy TCS SP5 and excited using 488 nM wavelength laser emission. All assays were performed in triplicate and it was done three repetitions for each cell sample and experimental condition.

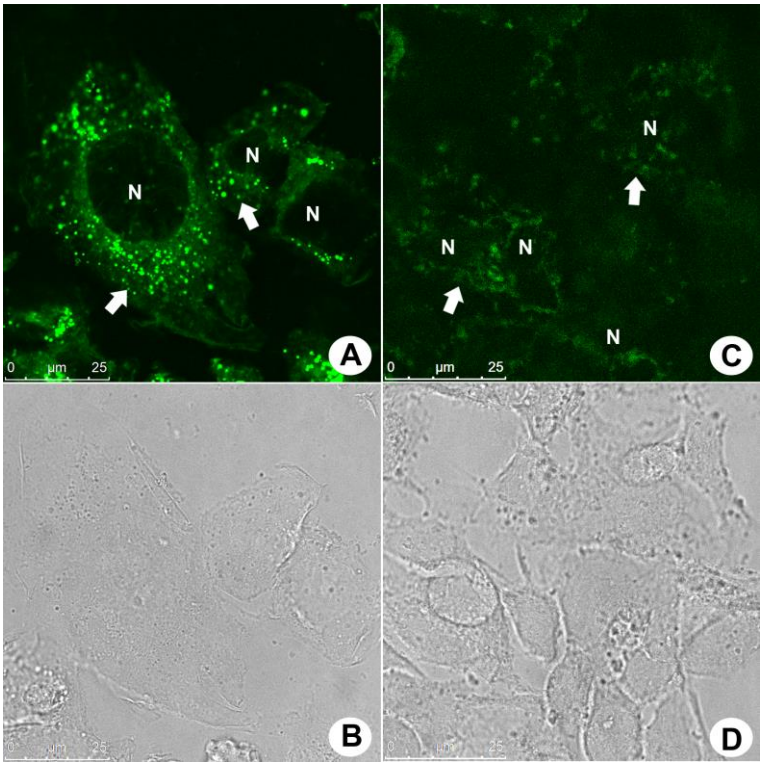

Figure S56. Fixed caco-2 cell lineages stained with **P4** (10 μM) and commercial available BODIPY. (A) Lipid droplets stained with BODIPY. (B) Cells stained with **P4** showing its accumulation in the lipid droplets (white arrows). (C) and (D) show the normal morphological aspects of the samples by phase. N = nucleus and scale bar of 25 μM.

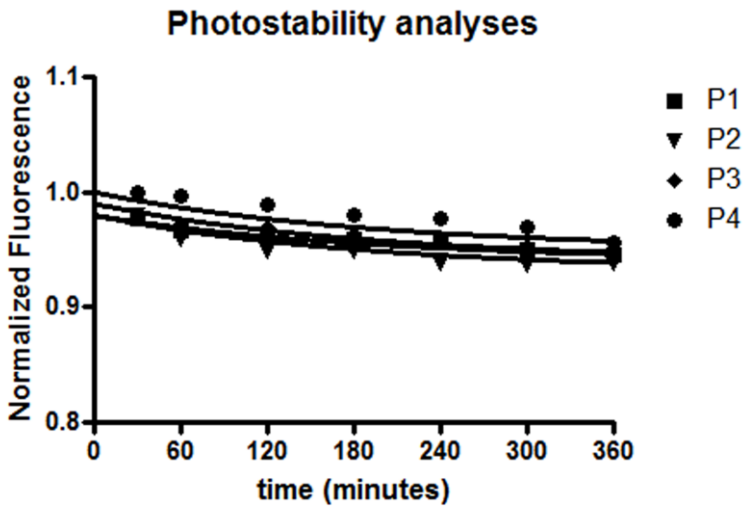

Figure S57. Photostability analyses for P1-P4 during a period of 6 hours.

Table S6. Water/n-octanol partition coefficients estimated in DFT and semi-empirical levels of theory.

Compounds	B3LYP/6-31+G(d)/PCM		AM1/PCM	
	Dipole (Debye)	Log P[1]	Dipole (Debye)	Log P[1]
P1	4.53	-0.87	4.05	-0.87
P2	4.08	-1.15	3.69	-1.16
P3	6.11	-0.98	4.34	-0.65
P4	7.09	-1.24	4.69	-1.19

[1] $Log(P) = \frac{\Delta G(water) - \Delta G(n-octanol)}{2.303\ R\ T}$; T=298.15 K.

1. Williams, A. T. R.; Winfield, S. A.; Miller, J. N.; *Analyst* **1983**, *108*, 1067-1071.

2. Melhuish, W. H. J.; *Phys. Chem.***1961**, *65*, 229-235.

3. Owen, T.; Fundamentals of modern UV-visible spectroscopy. (2000) Agilent Technologies.

4. Umberger, J. Q.; LaMer, V. K.; *J. Am. Chem. Soc.*, **1945**, *67*, 1099-1109.

5. Frisch, M. J.; Trucks, G. W.; Schlegel, H. B.; Scuseria, G. E.; Robb, M. A.; Cheeseman, J. R.; Scalmani, G.; Barone, V.; Mennucci, B.; Petersson, G. A.; Nakatsuji, H.; Caricato, M.; Li, X.; Hratchian, H. P.; Izmaylov, A. F.; Bloino, J.; Zheng, G.; Sonnenberg, J. L.; Hada, M.; Ehara, M.; Toyota, K.; Fukuda, R.; Hasegawa, J.; Ishida,

M.; Nakajima, T.; Honda, Y.; Kitao, O.; Nakai, H.; Vreven, T.; Montgomery Jr., J. A.; Peralta, J. E.; Ogliaro, F.; Bearpark, M. J.; Heyd, J.; Brothers, E. N.; Kudin, K. N.; Staroverov, V. N.; Kobayashi, R.; Normand, J.; Raghavachari, K.; Rendell, A. P.; Burant, J. C.; Iyengar, S. S.; Tomasi, J.; Cossi, M.; Rega, N.; Millam, N. J.; Klene, M.; Knox, J. E.; Cross, J. B.; Bakken, V.; Adamo, C.; Jaramillo, J.; Gomperts, R.; Stratmann, R. E.; Yazyev, O.; Austin, A. J.; Cammi, R.; Pomelli, C.; Ochterski, J. W.; Martin, R. L.; Morokuma, K.; Zakrzewski, V. G.; Voth, G. A.; Salvador, P.; Dannenberg, J. J.; Dapprich, S.; Daniels, A. D.; Farkas, Ö.; Foresman, J. B.; Ortiz, J. V.; Cioslowski, J.; Fox, D. J. *Gaussian 09*, Gaussian, Inc.: Wallingford, CT, USA, 2009.

6. Perdew, J. P.; Burke, K.; Ernzerhof, M.,Generalized Gradient Approximation Made Simple *Phys. Rev. Lett.* **1996**, *77*, 3865-3868.
7. Perdew, J. P.; Burke, K.; Ernzerhof, M.,Generalized Gradient Approximation Made Simple (Vol 77, Pg 3865, 1996) *Phys. Rev. Lett.* **1997**, *78*, 1396-1396.
8. Dunning, T. H.,Gaussian-Basis Sets for Use in Correlated Molecular Calculations .1. The Atoms Boron through Neon and Hydrogen *J. Chem. Phys.* **1989**, *90*, 1007-1023.
9. Tomasi, J.; Mennucci, B.; Cammi, R., Quantum Mechanical Continuum Solvation Models *Chem. Rev.* **2005**, *105*, 2999-3093.